Available online at www.sciencedirect.com
SCIENCE DIRECT
Lithos 79 (2005) 425–452
LITHOS
www.elsevier.com/locate/lithos

Geochemistry and petrogenesis of basalts from the West Siberian Basin: an extension of the Permo–Triassic Siberian Traps, Russia

Marc K. Reichow[a,*], A.D. Saunders[a], R.V. White[a], A.I. Al'Mukhamedov[b], A.Ya. Medvedev[b]

[a]*Department of Geology, University of Leicester, University Road, Leicester LE1 7RH, UK*
[b]*Institute of Geochemistry, Favorsky Street, Post Office Box 4019, Irkutsk 664033, Russia*

Received 11 December 2003; accepted 9 September 2004
Available online 18 November 2004

Abstract

New major and trace element data for the Permo–Triassic basalts from the West Siberian Basin (WSB) indicate that they are strikingly similar to the Nadezhdinsky suite of the Siberian Trap basalts. The WSB basalts exhibit low Ti/Zr (~50) and low high-field-strength element abundances combined with other elemental characteristics (e.g., low Mg#, and negative Nb and Ti anomalies on mantle-normalised plots) typical of fractionated, crustally contaminated continental flood basalts (CFBs). The major and trace element data are consistent with a process of fractional crystallisation coupled with assimilation of incompatible-element-enriched lower crust. Relatively low rates of assimilation to fractional crystallisation (~0.2) are required to generate the elemental distribution observed in the WSB basalts. The magmas parental to the basalts may have been derived from source regions similar to primitive mantle (OIB source) or to the Ontong Java Plateau source. Trace element modelling suggests that the majority of the analysed WSB basalts were derived by large degrees of partial melting at pressures less than 3 GPa, and therefore within the garnet-spinel transition zone or the spinel stability field.

It seems unlikely that large-scale melting in the WSB was induced through lithospheric extension alone, and additional heating, probably from a mantle plume, would have been required. We argue that the WSB basalts are chemically and therefore genetically related to the Siberian Traps basalts, especially the Nadezhdinsky suite found at Noril'sk. This suite immediately preceded the main pulse of volcanism that extruded lava over large areas of the Siberian Craton. Magma volume and timing constraints strongly suggest that a mantle plume was involved in the formation of the Earth's largest continental flood basalt province.

Keywords: West Siberian Basin basalts; Siberian Traps; Mantle plume; Continental flood basalt; Large igneous province; Nadezhdinsky suite

1. Introduction

The origins of large igneous provinces (LIPs), and especially continental flood basalts (CFBs), are still hotly debated. Many workers (e.g., Richards et al.,

* Corresponding author. Tel.: +44 116 252 3912; fax: +44 116 252 3918.
E-mail address: mkr6@le.ac.uk (M.K. Reichow).

0024-4937/$ - see front matter © 2004 Elsevier B.V. All rights reserved.
doi:10.1016/j.lithos.2004.09.011

1989; White and McKenzie, 1989; Campbell and Griffiths, 1990) invoke mantle plumes in their formation, whereas others (e.g., Anderson, 1994; King and Anderson, 1995, 1998) reject this, arguing instead for lithospherically controlled melting processes. The debate has been especially intense in the case of the Permo–Triassic Siberian Traps, which are not only the world's largest known CFB, but have also been implicated in the end-Permian mass extinction event. Most workers have proposed that a plume must have been responsible for the Traps (Renne and Basu, 1991; Sharma et al., 1992; Wooden et al., 1993), but others (e.g., Czamanske et al., 1998), have argued otherwise.

The present day outcrop of the Siberian Traps is located mainly on the Siberian Craton (Fig. 1). The dominant rock type is tholeiitic basalt with subordinate alkaline basalt. Basaltic rocks have also been recovered from industrial boreholes and reported from seismic sections from the West Siberian Basin (WSB). Russian geologists have previously proposed that these basalts represent a buried extension of the Siberian Traps (Zolotukhin and Al'Mukhamedov, 1988; Westphal et al., 1998; Al'Mukhamedov et al.,

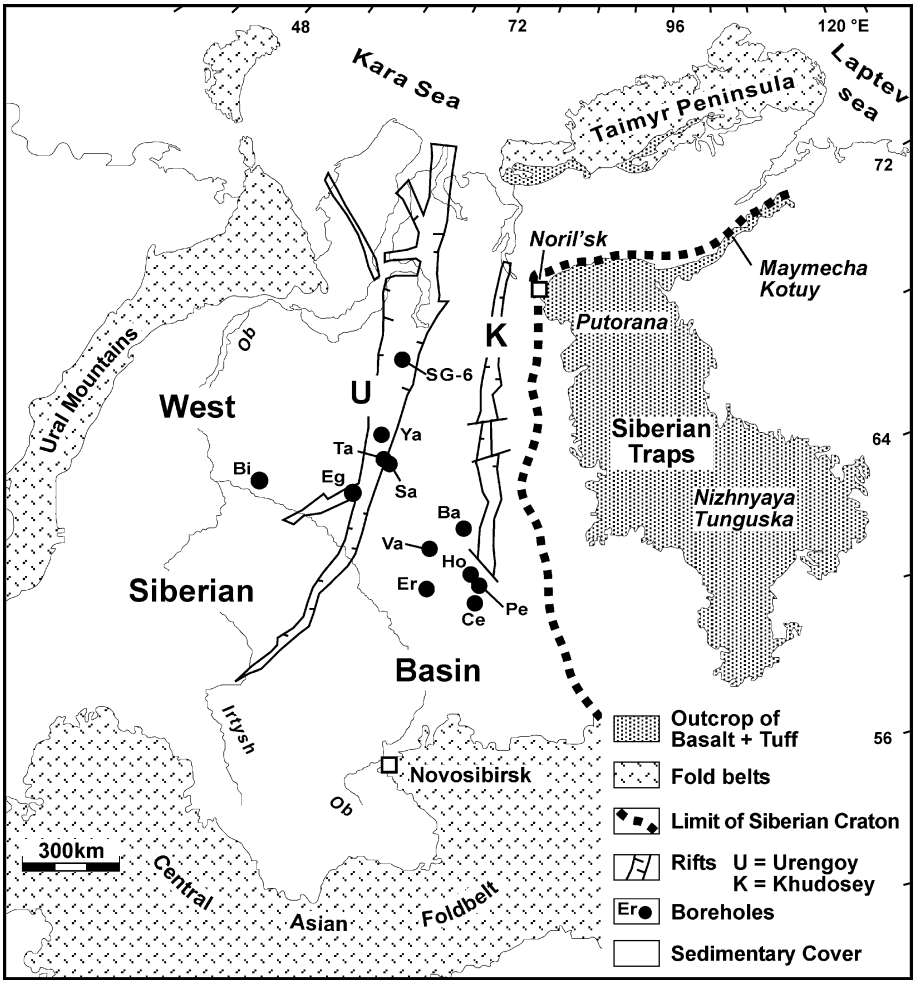

Fig. 1. Simplified geological map of the West Siberian Basin and surrounding areas. Locations of boreholes yielding basalt used in this study are shown by closed circles. Abbreviations are as follows: Ba=Bahilovskaya, Bi=Bistrinskaya, Ce=Chendih-Eganskaya, Eg=Egur'yahskaya, Er=Ershovaya, Ho=Hohryakovskaya, Pe=Permyakovskaya, Sa=Saem-Tahskaya, SG-6=Tjumen Superdeep, Ta=Tagrinskaya, Va=Van-Eganskaya, Ya=Yaraynerskaya.

1999; Medvedev et al., 2003), or possibly represent old oceanic crust (Aplonov, 1988, 1995). Reichow et al. (2002) recently showed that some basalts from the WSB are contemporaneous with the volcanic activity on the Siberian Craton at around 250 Ma, thereby confirming that the igneous province is substantially larger than previously estimated. However, it still remains unclear if the formation of the WSB basalts is related to rifting (Ziegler, 1992; Al'Mukhamedov et al., 1999) or is directly linked to the formation of the Siberian volcanic rocks to the east.

We have obtained over 60 basaltic samples from 12 different industrial boreholes in the WSB (Fig. 1). The boreholes were drilled for oil exploration and cores were taken only at some depth intervals. Therefore, no continuous lithostratigraphy could be obtained from cores. The extent of alteration of the sample material varies from slight to severe, where primary igneous minerals are replaced entirely. In this contribution, we present new major and trace element data for a selection of 32 of the least altered samples. These data are used for geochemical modelling and are compared with published data from the Siberian Traps to provide evidence for a relationship between the two volcanic regions. The basalts typically exhibit major and trace element compositions that differ substantially from ocean island basalts (OIB) and normal (N-) MORB. These differences cannot be explained solely by variations in partial melting or crystal fractionation, implying a contribution from the continental lithospheric mantle or continental crust. It is the aim of this paper to identify the processes that are responsible for the chemical characteristics of the WSB basalts, and determine whether or not a plume was involved in their formation. A companion paper (Saunders et al., 2005) presents an assessment of the Permo–Triassic uplift and extension in the WSB and argues that a mantle thermal anomaly, such as a plume, is a prerequisite for the formation of the basalts in the WSB and on the Siberian Craton.

2. Geological and tectonic setting

The WSB is one of the largest sedimentary basins in the world, covering an area of about 3.5×10^6 km^2 (Fig. 1). It is located between the Siberian Craton and the Ural Mountains and contains thick sequences of Permo–Triassic volcanic rocks, Triassic continental rocks and Jurassic to Cenozoic continental and marine sedimentary rocks (Peterson and Clarke, 1991; Westphal et al., 1998). The Mesozoic and Cenozoic sedimentary cover is up to 10 km thick in the north but thins towards the south and towards the margins of the basin (Peterson and Clarke, 1991; Saunders et al., 2005). These volcanic and sedimentary rocks rest on a complex basement comprising deformed and undeformed sediments and crystalline rocks of Palaeozoic and Proterozoic age (e.g., Peterson and Clarke, 1991; Aplonov, 1995; Bochkarev et al., 2003). The basement is heavily faulted, producing long, roughly N–S trending rifts (for example, the Urengoy and Khudosey rifts: Fig. 1). Different distributions of these rifts are presented in the literature (e.g., Zonenshain et al., 1990; Surkov, 1995) and in Fig. 1 the version of Al'Mukhamedov et al. (1999) is presented. The timing of onset of rifting cannot unequivocally be resolved. Rifting is thought to have begun in the Permian, but continued into the Triassic and at least in part post-dates the basaltic magmatism (Saunders et al., 2005).

The Permo–Triassic igneous rocks underlie the Mesozoic sedimentary succession and consist mainly of basalts and gabbros with rare rhyolites. Most of the drilled volcanic rocks were recovered from the rift grabens, but some occur on the rift flanks. From seismic studies and deep borehole data (Westphal et al., 1998), the volcanic sequences in the northern portions of the rifts are in places as much as 2 km thick. Basalts comprise the vast majority (>90%) of samples recovered by industrial drilling with plagioclase-phyric basalts and dolerites, amygdaloidal basalts, basaltic breccias and tuffs being present. Gabbros are found in the Van-Eganskaya borehole (Va, Fig. 1) and are reported from the super-deep borehole SG-6 (Westphal et al., 1998). Rhyolite occurs in the central part of the WSB (Medvedev et al., 2003), but the proportion appears to be small (unlike, for example, the Paraná province: Hawkesworth et al., 2000).

3. Sampling and petrography

Basalt samples obtained for this study are from 12 industrial boreholes. Four boreholes are located in the

Urengoy rift and two on the rift flanks (Fig. 1 and Table 1). A further six of the boreholes border the Khudosey rift to the west and southwest. Generally, samples were taken from a depth of between 2620 and 4340 m below surface although one sample was taken at 7006 m below surface in borehole SG-6. Sampling intervals range from 147 to 898 m, but for some boreholes only one sample was available. Wherever possible, samples were taken from the centre of the most massive lava flows to obtain the least altered basalt. Unfortunately, detailed borehole log data is only available for the Permyakovskaya borehole

Table 1
Borehole locations of the WSB basalts and sample characteristics

Borehole	Latitude/ longitude	Sample no.	Depth below surface (m)	Rock type	Rock texture	Phenocryst phase[a]	(Modal proportion)[b]
Khudosey rift							
Permyakovskaya	60°30′ N	97-7	2838.4	basalt	porphyritic	plag	5–7%
	86°00′ E	97-8	2865.3	basalt	porphyritic	plag	10%
		97-12	2869.7	basalt	porphyritic	plag	3–5%
		97-22	2951.6	basalt	porphyritic	plag	7–10%
		97-24	2955.8	basalt	porphyritic	plag	3–5%
		97-26	2959.0	basalt	porphyritic	plag	3–5%
		97-27	2980.6	dolerite	subophitic	–	–
		97-39	2981.0	dolerite	ophitic	–	–
		97-40	2983.0	basalt	porphyritic	plag	5–10%
		97-45	2985.5	dolerite	poikilophitic	cpx/plag	7–10%
Van-Eganskaya	61°30′ N	97-79	3241.8	basalt	porphyritic	plag	4%
	82°20′ E						
Hohryakovskaya	60°50′ N	97-97	2797.1	basalt	porphyritic	plag/ol	10%
	85°40′ E	95-56	2797.2	basalt	porphyritic	plag/ol	15%
		97-96	2797.4	basalt	porphyritic	plag/ol	10%
Bahilovskaya	61°40′ N	97-71	3552.6	basalt	porphyritic	cpx	7–10%
	84°30′ E						
Chendih-Eganskaya	59°40′ N	95-41	2629.1	basaltic-andesite	aphyric	–	–
	85°50′ E						
Ershovaya	60°20′ N	95-49	3102.2	basalt	porphyritic	plag	3%
	83°20′ E						
Urengoy rift							
Yaraynerskaya	63°50′ N	95-13	3201.0	basalt	porphyritic	plag	7–10%
	77°50′ E	95-15	4074.0	basalt	porphyritic	plag	7–10%
		95-16	4086.5	basalt	poikilophitic	plag/cpx	–
		95-17	4099.5	basalt	poikilophitic	plag/cpx	–
Bistrinskaya	61°24′ N	95-18	2904.8	basalt	poikilophitic	plag/cpx	–
	69°36′ E						
Tagrinskaya	63°20′ N	95-39	3537.0	basalt	porphyritic	plag	7–10%
	78°00′ E	95-36	4251.7	basalt	poikilophitic	plag/cpx	–
		95-37	4339.0	basalt	poikilophitic	plag/cpx	–
SG-6	66°00′ N	96-3	7006.4	basalt	porphyritic	plag	5–7%
	77°00′ E						
Saem-Tahskaya	63°15′ N	95-58	4140.0	basalt	aphyric	–	–
	78°30′ E	97-60A	4288.7	–	–	–	–
		97-61B	4292.6	basalt	poikilophitic	plag/cpx	–
		97-62	4297.9	basalt	poikilophitic	plag/cpx	–
		97-63	4303.6	basalt	poikilophitic	plag/cpx	–
Egur'yahskaya	61°10′ N	95-35	3626.0	dolerite	ophitic	plag/cpx	–
	76°50′ E						

[a] Abbreviations are as follows: plag=plagioclase, cpx=clinopyroxene, ol=olivine.
[b] Percentage of phenocrysts (total).

where about 41% of the drilled basaltic section was recovered (Fig. 2).

In the Permyakovskaya borehole, the lithological units range in thickness from 0.3 to 45 m. The lava flows have a vesicular brecciated top and a massive interior, features typical of thick sub-aerial lava flows (Self et al., 1998). This characteristic is also picked up by down-hole logging data, which allow a continuous reconstruction of the lithologies (Al'Mukhamedov, unpublished data). Sub-metre-thick tuff layers are

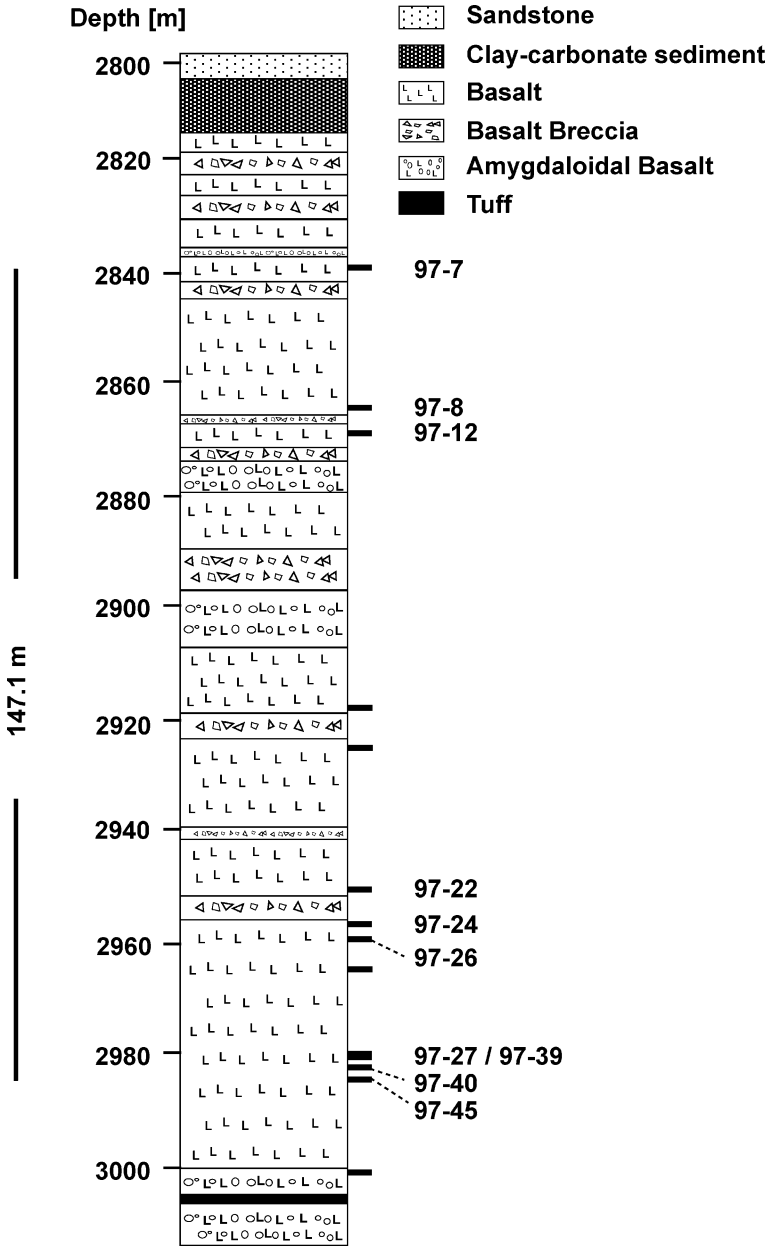

Fig. 2. Lithological log of the Permyakovskaya borehole showing the petrography and sampling intervals of the WSB basalts. At least some of the basalts are effusive as indicated by brecciated and vesicle-rich flows. Positions of 10 analysed samples are indicated on the right-hand side of the column.

Table 2
Major (in wt.%) and trace element (in ppm) data for the WSB basalts close to the Khudosey rift

Borehole	Permyakovskaya										Van-Eganskaya	Hohryakovskaya			Bahilovskaya	Chendih-Eganskaya	Ershovaya
Sample no.	97-7	97-8	97-12	97-22	97-24	97-26	97-27	97-39	97-40	97-45	97-79	97-97	95-56	97-96	97-71	95-41	95-49
Depth	2838.4	2865.3	2869.7	2951.6	2955.8	2959.0	2980.6	2981.0	2983.0	2985.5	3241.8	2797.1	2797.2	2797.4	3552.6	2629.1	3102.2
SiO_2 (wt.%)	54.43	49.96	46.59	54.71	49.69	51.38	50.55	50.47	50.79	49.97	47.87	51.13	50.97	51.52	47.97	58.86	50.03
TiO_2	1.23	1.54	1.39	1.12	1.12	1.14	1.08	1.06	1.11	1.05	1.25	1.24	1.20	1.25	0.71	1.30	1.26
Al_2O_3	18.25	17.80	17.13	18.02	17.64	17.89	17.00	16.90	17.67	17.49	19.16	16.36	16.08	16.54	16.12	17.07	17.25
$Fe_2O_{3(tot)}$	10.54	11.96	13.39	11.17	10.76	13.20	11.41	11.48	10.41	11.42	10.94	12.04	11.73	10.93	10.70	9.09	11.89
MgO	3.43	3.14	6.08	5.51	5.19	6.37	5.76	5.82	5.27	5.77	3.72	4.39	5.77	4.60	9.98	3.60	6.20
CaO	7.42	9.37	10.63	4.52	10.39	6.29	8.93	8.97	9.35	9.11	12.63	9.48	9.07	9.83	11.24	5.92	9.91
Na_2O	3.63	3.33	2.89	3.81	3.43	2.71	3.39	3.44	3.52	3.40	3.16	3.31	3.13	3.27	2.11	3.07	2.51
K_2O	0.49	2.17	1.25	0.73	1.25	0.59	1.37	1.35	1.39	1.27	0.59	1.34	1.38	1.37	0.80	0.35	0.45
P_2O_5	0.46	0.58	0.50	0.36	0.36	0.36	0.35	0.34	0.35	0.34	0.33	0.48	0.46	0.51	0.15	0.67	0.33
MnO	0.11	0.15	0.14	0.06	0.17	0.06	0.16	0.16	0.14	0.17	0.34	0.22	0.21	0.19	0.22	0.06	0.18
LOI	6.16	6.11	5.71	5.60	5.91	4.80	3.06	3.01	4.17	3.09	5.90	4.83	3.71	4.82	2.80	4.37	5.81
Mg#[a]	42.3	37.1	50.5	52.6	52.0	52.0	53.2	53.3	53.2	53.2	43.4	50.6	52.9	53.0	67.7	47.6	54.4
Eu/Eu*[a]	0.93	0.86	0.87	0.73	0.71	0.78	0.84	0.72	0.87	0.89	1.01	0.83	0.88	0.92	1.12	0.91	0.83
Ba (ppm)	612	1020	802	531	597	470	582	554	644	574	347	887	836	902	242	680	447
Cr	22	7	4	31	29	29	26	26	24	25	27	25	25	39	360	138	71
Cu	16	24	24	54	25	35	41	43	47	58	45	23	27	24	32	20	92
Nb	10.5	16.8	10.2	17.0	17.2	17.8	17.4	16.8	16.5	15.3	6.2	8.4	8.9	9.4	4.0	10.7	6.1
Ni	30.8	19.7	33.6	80.6	85.5	77.2	83.0	85.4	66.8	82.0	63.3	42.2	40.8	38.8	153	108	96.2
Rb	11	54	23	39	70	33	80	77	79	68	11	27	27	27	26	6	8
Sc	25	20	27	27	25	29	23	23	23	23	35	25	24	27	36	29	39
Sr	768	1317	1006	533	839	653	697	653	861	695	565	873	802	894	447	772	549
V	128	104	136	140	147	155	139	134	147	139	184	182	182	187	172	193	222
Y	30.0	45.3	38.6	41.8	50.8	40.5	49.5	47.6	49.4	46.9	39.8	35.6	34.1	35.9	26.2	31.0	34.6
Zn	94	135	138	119	116	119	116	113	108	106	121	109	108	94	82	78	99
Zr	141	223	169	128	121	130	124	120	123	119	142	146	145	147	87	167	126
La	22.10	30.96	23.42	13.82	18.09	16.54	18.35	17.79	17.06	16.25	15.55	27.83	35.00	28.16	13.0	37.56	20.37
Ce	50.43	71.07	54.67	33.11	36.57	37.26	41.00	40.56	41.89	39.18	36.78	60.87	70.00	61.82	24.0	85.27	44.55
Pr	6.08	7.54	6.69	4.22	4.78	4.25	4.91	4.82	5.53	4.46	4.56	6.47	7.20	7.29	–	9.70	5.47
Nd	27.78	28.97	27.79	18.74	22.39	22.17	19.90	24.32	23.49	19.40	18.44	24.85	32.00	28.63	15.0	37.97	21.68
Sm	5.95	6.68	6.77	4.93	5.78	5.12	5.06	6.60	5.89	4.88	4.43	6.58	7.10	7.06	4.0	7.11	4.58
Eu	1.61	1.96	1.86	1.18	1.34	1.29	1.45	1.48	1.78	1.46	1.50	1.80	1.90	1.95	1.4	1.99	1.35
Gd	4.72	7.18	6.26	4.93	5.78	5.04	5.44	5.91	6.56	5.19	4.61	6.66	6.10	5.90	3.6	6.30	5.27
Dy	4.59	6.94	6.32	5.61	7.59	5.37	6.54	6.73	7.44	6.25	5.20	5.81	5.20	5.67	4.4	4.41	4.61
Er	2.82	3.82	3.78	3.52	4.90	3.53	3.86	4.47	4.83	3.73	3.05	3.49	2.90	3.25	2.6	2.44	2.86
Yb	2.74	3.64	3.18	3.28	4.97	3.61	3.99	4.66	4.56	4.00	3.37	2.89	3.20	3.00	3.7	2.06	2.56
Lu	0.47	0.57	0.50	0.51	0.86	0.61	0.64	0.77	0.72	0.59	0.51	0.46	0.53	0.46	0.6	0.28	0.38
Nb/Zr	0.07	0.08	0.06	0.13	0.14	0.14	0.14	0.14	0.13	0.13	0.04	0.06	0.06	0.06	0.05	0.06	0.05
Nb/Y	0.35	0.37	0.26	0.41	0.34	0.44	0.35	0.35	0.33	0.33	0.16	0.23	0.26	0.26	0.15	0.34	0.18
$(La/Sm)_{C1}$[a]	2.32	2.89	2.16	1.75	1.95	2.02	2.27	1.68	1.81	2.08	2.19	2.64	3.08	2.49	2.03	3.30	2.78

Major (in wt.%) and trace element (in ppm) data for the WSB basalts within or close to the Urengoy rift. SG-6=Tjumen superdeep borehole

Borehole	Yaraynerskaya				Bistrinskaya	Tagrinskaya			SG-6	Saem-Tahskaya					Egur'yahskaya
Sample no.	95-13	95-15	95-16	95-17	95-18	95-39	95-36	95-37	96-3	95-58	97-60A	97-61B	97-62	97-63	95-35
Depth	3201.0	4074.0	4086.5	4099.5	2904.8	3537.0	4251.7	4339.0	7006.4	4140.0	4288.7	4292.6	4297.9	4303.6	3626.0
SiO_2 (wt.%)	49.05	49.36	49.04	48.69	53.63	52.89	49.29	51.01	45.46	50.41	50.93	50.77	50.30	49.66	47.26
TiO_2	1.27	0.88	1.01	1.27	0.91	1.31	0.96	0.91	2.13	1.46	1.30	1.00	0.98	0.99	0.69
Al_2O_3	15.56	18.24	16.82	15.42	16.74	15.66	16.82	17.06	18.11	15.07	15.94	16.71	16.74	17.11	16.96
$Fe_2O_{3(tot)}$	13.18	10.77	11.87	13.30	8.48	11.73	11.43	10.62	15.55	15.18	12.35	11.79	11.76	11.60	10.79
MgO	6.76	8.52	8.75	7.11	7.42	5.59	8.00	7.74	10.43	4.72	6.61	7.19	7.57	7.01	11.61
CaO	10.28	7.86	7.93	10.23	8.38	6.82	10.06	8.55	2.53	7.06	6.42	6.62	7.39	9.28	9.88
Na_2O	2.96	3.13	3.32	3.05	3.08	3.27	2.43	2.98	4.02	4.17	4.11	3.74	3.92	3.55	2.21
K_2O	0.56	0.87	0.85	0.59	1.05	2.06	0.61	0.71	1.08	1.45	1.83	1.75	0.90	0.37	0.31
P_2O_5	0.16	0.19	0.22	0.15	0.25	0.49	0.22	0.24	0.38	0.28	0.34	0.24	0.23	0.23	0.13
MnO	0.20	0.18	0.19	0.20	0.06	0.18	0.18	0.18	0.31	0.19	0.18	0.20	0.20	0.19	0.15
LOI	2.74	5.19	5.50	2.66	4.97	3.29	5.03	3.85	5.57	2.35	3.80	3.82	3.50	4.14	2.30
Mg#[a]	53.6	64.0	62.4	54.6	66.3	51.7	61.2	62.1	60.1	41.1	54.6	57.8	59.1	57.6	70.8
Eu/Eu*[a]	0.86	0.88	0.89	0.95	0.79	0.87	0.85	0.88	0.98	0.85	0.91	0.89	0.86	1.08	0.83
Ba (ppm)	389	1020	647	303	437	1247	357	411	798	1376	1179	954	998	423	177
Cr	169	81	125	163	215	43	74	58	231	63	17	88	134	130	394
Cu	80	39	50	76	31	37	82	100	95	54	18	29	28	28	16
Nb	4.7	5.6	7.2	5.3	6.7	9.3	4.7	5.2	11.2	9.4	9.7	5.0	5.8	6.2	2.8
Ni	61.5	107	101	63.8	105	52.9	173.7	171.3	96.8	36.6	20.4	77.4	90.0	82.4	44.0
Rb	10	14	10	12	17	37	8	16	12	22	28	39	15	5	6
Sc	38	30	29	34	33	29	27	29	39	35	26	29	29	33	24
Sr	354	564	501	350	416	775	469	660	113	766	862	956	869	882	326
V	254	161	177	242	169	207	166	184	171	265	191	188	188	201	127
Y	32.6	28.1	33.3	33.4	26.8	43.4	32.7	29.6	31.8	47.8	40.2	32.1	31.8	31.2	17.8
Zn	102	87	94	103	77	114	89	86	151	124	122	110	105	102	77
Zr	89	103	118	90	144	172	115	115	106	179	158	118	110	117	62
La	13.00	17.00	12.03	9.35	27.00	25.77	14.00	13.33	10.52	19.64	22.29	14.50	13.68	14.04	6.22
Ce	20.00	25.00	26.95	20.16	53.00	56.20	33.00	31.57	21.93	44.83	51.58	36.54	35.47	32.57	16.58
Pr	2.70	3.40	3.55	2.41	5.00	7.20	3.60	3.42	2.88	4.82	5.90	4.43	4.60	3.83	2.11
Nd	12.00	14.00	15.56	11.61	20.00	33.52	16.00	15.61	13.80	20.60	25.23	18.41	18.63	16.14	10.54
Sm	3.40	3.20	3.87	3.50	4.30	7.42	4.20	4.10	4.01	5.34	6.26	4.17	4.27	4.22	3.41
Eu	1.10	1.00	1.16	1.22	1.10	1.97	1.20	1.16	1.23	1.61	1.81	1.23	1.20	1.48	0.88
Gd	4.50	3.80	4.11	4.44	4.20	6.43	4.40	3.91	3.64	6.25	5.85	4.24	4.28	4.17	3.05
Dy	5.00	3.90	4.42	5.12	3.50	6.21	4.60	3.95	3.71	6.90	6.20	4.04	4.08	5.04	3.10
Er	3.20	2.30	2.86	3.10	2.00	3.86	2.80	2.30	2.07	4.16	3.34	2.48	2.51	2.92	1.77
Yb	3.30	2.60	2.51	2.96	2.10	3.69	3.30	2.45	1.87	4.02	3.57	2.71	2.74	2.82	1.66
Lu	0.51	0.37	0.37	0.47	0.31	0.63	0.55	0.36	0.25	0.62	0.55	0.45	0.45	0.45	0.26
Nb/Zr	0.05	0.05	0.06	0.06	0.05	0.05	0.04	0.04	0.11	0.05	0.06	0.04	0.05	0.05	0.05
Nb/Y	0.14	0.20	0.22	0.16	0.25	0.21	0.14	0.17	0.35	0.20	0.24	0.16	0.18	0.20	0.16
$(La/Sm)_{C1}$[a]	2.39	3.32	1.94	1.67	3.92	2.08	2.03	2.17	1.64	2.30	2.22	2.17	2.00	2.08	1.14

[a] Mg#=[100×(MgO/FeO+MgO)] assuming Fe_2O_3/FeO of 0.15; Eu/Eu* calculated with $Eu^*=10^{[0.5\times\log(Sm\times Gd)]}$; C1 postscript denotes chondrite 1 after McDonough and Sun (1995). Note all major element data are recalculated volatile-free.

recorded from the bottom of Permyakovskaya borehole, but the absence of non-volcanic sedimentary rocks in this borehole is striking. The occurrence of gabbroic rocks in some boreholes (Westphal et al., 1998; Reichow et al., 2002) suggests that some units are intrusive or alternatively represent the centres of massive lava flows (e.g., Permyakovskaya).

Most WSB basalts contain phenocrysts of plagioclase±clinopyroxene±olivine with plagioclase as the main phenocryst phase for all basalts, indicating shallow crystallisation levels (see Table 1). Subophitic texture, with small plagioclase needles intergrown with clinopyroxene, is observed in several thin sections from the Permyakovskaya borehole and indicates near-eutectic crystallisation conditions for these rocks. Rare olivine phenocrysts show signs of resorption. Alteration of the rocks is manifested by partial to complete replacement of plagioclase by sericite, of glass by chlorite and of olivine by iddingsite; by the infilling of vesicles with ankerite and calcite; and by the presence of veins and patches of chlorite and carbonates. The extent of alteration varies from slight to severe, where phenocrysts remain only as relict forms or hand specimens appear green due to chloritization.

4. Analytical procedures

Samples were prepared for analysis by grinding in an agate Tema mill. Major element data were obtained on fusion beads by X-ray fluorescence analysis using a multi-component XR-spectrometer CPM-25 (Russian model) at the Institute of Geochemistry, Irkutsk, Russia. Details of the analytical procedures and applied corrections on matrix effects are available in Afonin et al. (1984). Total loss on ignition (LOI) was measured on powders that had been pre-dried at 120 °C for at least 12 h. Powders were ignited at 950 °C in air for 1 h, before cooling and reweighing.

Trace element data were obtained on powder pellets by XRF at the University of Leicester using standard methods as described by Harvey et al. (1996). To improve precision for elements such as Ba, Rb, Nb, Ni, V, Y and Zr, these elements were determined by XRF using long counting times; this procedure both lowered the detection limits (Ba 4 ppm, Rb 0.5 ppm, Nb 0.4 ppm, Ni 0.8 ppm, V 1 ppm,

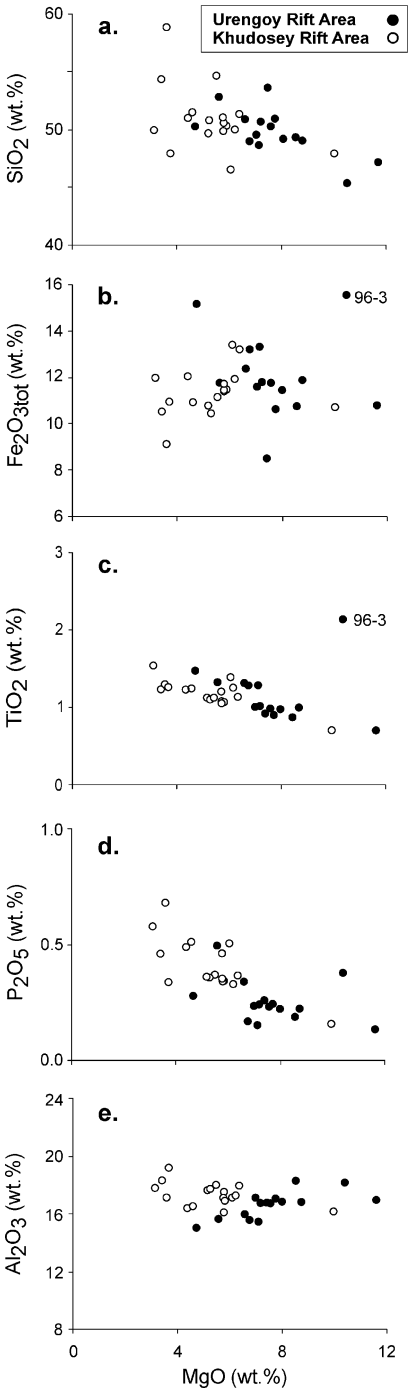

Fig. 3. Major element data (wt.%) versus MgO (wt.%) for basalt samples from the West Siberian Basin. Data recalculated on a volatile-free basis. High TiO_2 and $Fe_2O_{3(tot)}$ in SG-6 sample 96-3 probably indicate abundant chlorite.

Y 0.5 ppm, Zr 0.5 ppm) compared to normal counting statistics and resulted in a precision better than 1%. Calibrations were set using internal and international rock reference material (e.g., BCR-1, BHVO-1, W-2).

Rare earth elements (REE) were pre-concentrated using ion exchange columns; these solutions were then analysed on a JY-Ultima-2 inductively coupled optical emission spectrometer at the University of Leicester, UK. Calibration was carried out using internal and international geochemical reference material. Details of analytical procedures are given in Harvey et al. (1996).

Due to the high degree of alteration, all major element data are recalculated volatile-free for the purpose of this paper. Trace and major element modelling mainly focuses on relatively immobile elements (e.g., Zr, Ti, Nb and the REE), which are likely to be less affected by alteration. The only exception is the use of the more mobile element Ba, which will be considered and discussed in Section 6.3.

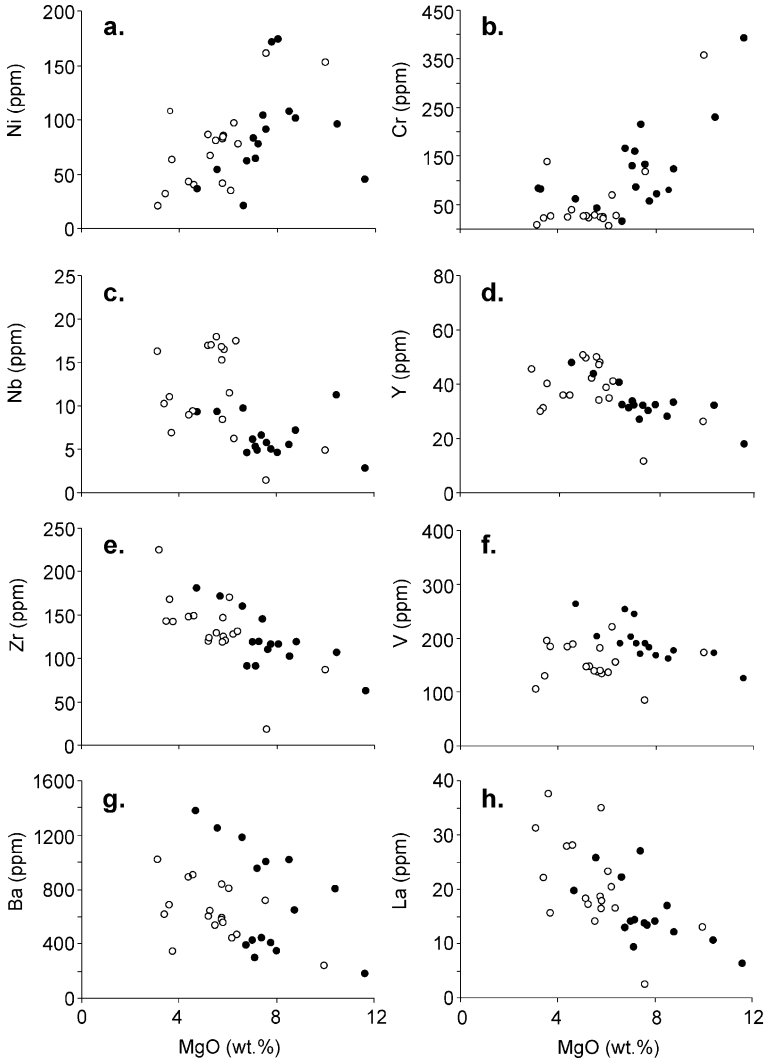

Fig. 4. Trace element data (ppm) versus MgO (wt.%) for basalt samples from the West Siberian Basin. MgO data recalculated on a volatile-free basis. Symbols as in Fig. 3.

5. Results

For convenience, in the succeeding diagrams, we have divided the dataset into two groups based on their geographical location: those recovered from within or close to the Urengoy rift (in the central part of the basin), and those close to the Khudosey rift, which is located close to the edge of the Siberian Craton (Fig. 1).

5.1. Major element compositions

Analyses of 32 representative samples are listed in Table 2 and illustrated in Fig. 3a–e. The principal major element characteristics recalculated on a volatile-free basis are variable MgO (3–12 wt.%; the majority <8 wt.%) and $Fe_2O_{3(tot)}$ (8–16 wt.%) contents, resulting in Mg numbers (Mg#=100MgO/FeO+MgO) between 37 and 71 (average=55). Most samples close to the Urengoy rift have higher MgO contents (>6 wt.%) than basalts close to the Khudosey rift (<6 wt.%). The high Mg# of few samples demonstrate eruption of primitive magmas, but the presence of pseudomorphed olivine phenocrysts in the analysed rocks suggests that the high Mg# do not necessarily indicate primitive liquids; we cannot rule out some olivine accumulation. The samples do not show strong iron enrichment on the alkalis–iron–magnesium (AFM) diagram (Medvedev et al., 2003), demonstrating a more calc-alkalic rather than tholeiitic trend (note, however, that this may in part be due to alteration).

The abundance of TiO_2 varies between 0.6 and 2.2 wt.%, and P_2O_5 is in the range 0.13–0.67 wt.%, with both oxides showing enrichment with decreasing MgO (Fig. 3c and d). Samples from higher borehole levels are in general elevated in TiO_2, P_2O_5 and $Fe_2O_{3(tot)}$ (Table 2). Both TiO_2 and $Fe_2O_{3(tot)}$ increase slightly with decreasing MgO, indicating that magnetite or titanomagnetite were not major fractionating phases (although in a following section we argue that small amounts of magnetite were fractionating at an early stage of magmatic evolution). SiO_2 varies between 45 and 59 wt.% (average=50 wt.%), but shows a correlation with MgO only for basalts near the Urengoy rift. Al_2O_3 for most samples is rather uniform and close to 17 wt.%, although Hohryakovskaya sample 97–79 has 19 wt.%. Chendih-Eganskaya sample 95-41 is an andesite with 58.86 wt.% SiO_2, Na_2O+K_2O of 3.4 wt.% and high P_2O_5 of 0.67 wt.%.

5.2. Trace element compositions

The WSB basalt trace element characteristics are illustrated in Fig. 4a–h. Ni and Cr abundances are

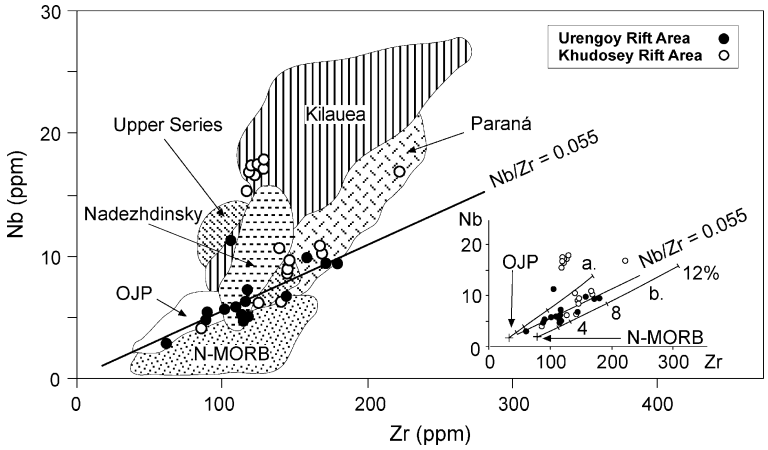

Fig. 5. Nb (ppm) versus Zr (ppm) for basalts from the West Siberian Basin in comparison with data for ocean island (Kilauea), normal mid-ocean-ridge basalt (N-MORB), the Siberian Nadezhdinsky suite and Upper Series basalts (note: Upper Series comprises five different sub-suites of similar trace element composition, see Table 3), Ontong Java Plateau (OJP) and Paraná basalt. The inset diagram illustrates fractional crystallisation coupled with small rates of assimilation (r=0.2) for primitive OJP (a) and N-MORB (b) magmas. Contaminant used for both trend lines is Bolgokhtokhsk granodiorite (Hawkesworth et al., 1995) with ticks on trend lines representing 2%, 4%, 8% and 12% assimilation. Data sources as in Fig. 6.

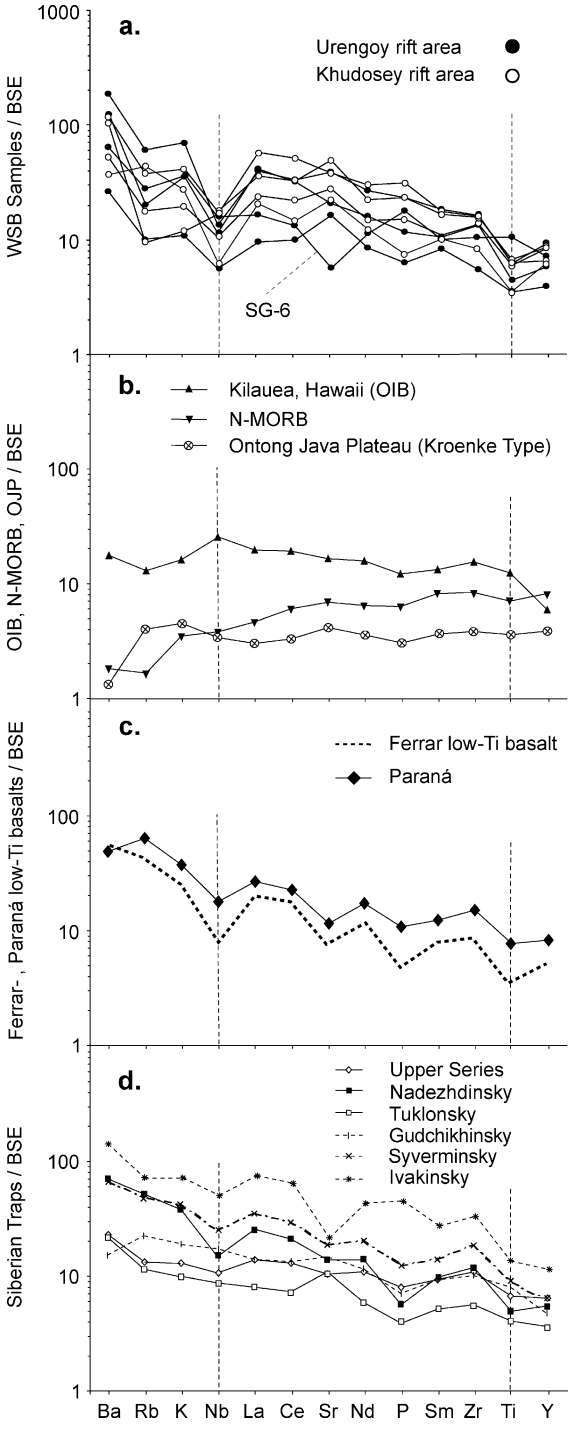

generally low, with averages around 80 and 91 ppm, respectively, consistent with the evolved nature of these samples indicated by the generally low Mg#. Samples with higher Mg# include the Bahilovskaya (Khudosey rift) and Egur'yahskaya (Urengoy rift) samples with Mg#=68 and 71, respectively. However, only the former sample displays both the high Ni (153 ppm) and Cr (360 ppm) consistent with a primitive magma composition, whereas the latter has high-Cr (394 ppm) but low-Ni (44 ppm) concentrations. The correlation between Ni, Cr and MgO (Fig. 4a and b) indicates, at least qualitatively, that both olivine and pyroxene fractionation have occurred. Cu ranges between 16 and 100 ppm but is low in most samples with an average of 44 ppm (Table 2).

Niobium (2–18 ppm), Y (17–51 ppm) and Zr (62–223 ppm) all show increases with decreasing MgO (Fig. 4c–e), as predicted by fractionation of plagioclase, olivine and clinopyroxene. The majority of the samples have Nb/Zr ratios of about 0.06, similar to ratios found in some ocean plateau basalts (e.g., Ontong Java Plateau, Mahoney et al., 1993; Fitton and Godard, 2004), although a small number of samples from Permyakovskaya borehole have significantly higher Nb/Zr, similar to basalts from Kilauea (e.g., Norman and Garcia, 1999; Fig. 5). All WSB basalts are light-REE-enriched relative to chondrite ($(La/Sm)_{C1}$=1.1–4.0, Table 2), and several show negative Eu anomalies. Eu/Eu* ratios of 0.7–1.2 (Table 2) indicate that plagioclase removal or accumulation occurred in at least some basalts.

Fig. 6a displays trace and minor element data for selected WSB samples normalised to bulk silicate earth (BSE: McDonough and Sun, 1995). All WSB basalts show high concentrations of large-ion-lithophile elements (Ba, Rb and K) relative to the more immobile elements (e.g., Zr, Ti and Y). There are pronounced negative anomalies at Nb and Ti, which is

Fig. 6. Bulk silicate earth normalised (BSE, after McDonough and Sun, 1995) multi-element diagram for representative basalt samples from: (a) the WSB; (b) ocean island basalt (Kilauea: Chen et al., 1996; Norman and Garcia, 1999), N-MORB (Saunders and Tarney, 1984; Salters and Stracke, 2004), average Ontong Java Plateau (Kroenke-type) basalt (Fitton and Godard, 2004); (c) Ferrar low-Ti basalts (Hergt et al., 1991; Brewer et al., 1992) and Paraná (Peate and Hawkesworth, 1996); (d) averaged data of the Siberian Traps suites (Lightfoot et al., 1990, 1993; Wooden et al., 1993; Hawkesworth et al., 1995).

a distinctive feature of some continental flood basalt provinces (e.g., low-Ti basalts of Ferrar, Hergt et al., 1991, and Paraná, Peate and Hawkesworth, 1996). The only exception to this pattern is sample 96-3 from the deepest section (7006.4 m) of borehole SG-6, which displays positive Ti and P anomalies and no Nb anomalies. The relative differences between the WSB basalts, ocean island basalts (Kilauea: Chen et al., 1996; Norman and Garcia, 1999), Ontong Java Plateau basalts (OJP: Fitton and Godard, 2004) and normal (N)-MORB (Saunders and Tarney, 1984; Salters and Stracke, 2004) are illustrated in Fig. 6b. The majority of the WSB basalts are elevated in large ion lithophile elements (LILE) and light REE, similar to or higher than OIB. Averaged N-MORB data generally display a lower abundance, except for Zr and Y, which are similar to the WSB data. The Ontong Java Plateau, the world's largest oceanic large igneous province, also shows low abundances of both Nb and Ti, although the abundances of other elements such as K, Ba and the light REE are much lower than in basalts from the WSB and indeed from many other continental LIPs (Saunders et al., 1992). The WSB data show similar element abundances to low-Ti basalts from the Ferrar and Paraná large igneous provinces (Fig. 6c).

The low-Ti abundances of the WSB basalts are illustrated on a plot of Ti versus Zr (Fig. 7). The majority of the WSB data have a near constant Ti/Zr ratio (51), similar to Ferrar, Paraná and the Noril'sk Nadezhdinsky suite basalts. This suggests similar conditions of formation, controlled by either the composition of the source, the nature of partial melting, the extent of contamination and/or the extent of titano-magnetite fractionation. These will be discussed in detail in Section 6.4.

6. Discussion

6.1. Effects of alteration and fractionation

The dated WSB basalts were erupted approximately 250 m.y. ago (Reichow et al., 2002) and were subsequently buried beneath a thick sedimentary cover. Thin section studies show variable amounts of secondary replacement of the primary igneous minerals (see Section 2, above). Element mobility, tested by plotting major and trace element data against LOI (not shown), reveals a high degree of mobility for K, Na, Rb and Sr, especially in samples with LOI>6.5 wt.%; accordingly, samples with LOI greater than 6.5 wt.% are not included in this paper. Permyakovskaya samples 97-7 and 97-8 are within 25–51 m of the Triassic sediment cover, respectively (Fig. 2), and have high LOIs (6.16 and 6.11 wt.%, respectively)

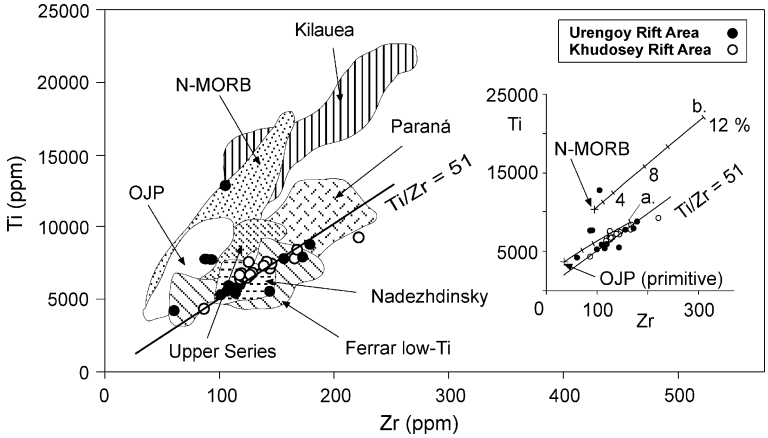

Fig. 7. Ti (ppm) versus Zr (ppm) for basalt from the WSB in comparison with data for ocean island (Kilauea), normal mid-ocean-ridge basalt (N-MORB), the Siberian Nadezhdinsky suite basalt, Ontong Java Plateau (OJP), Ferrar, Paraná and Upper Series basalt. The inset diagram illustrates fractional crystallisation coupled with small rates of assimilation (r=0.2) for primitive OJP (a) and N-MORB (b) magmas. Contaminant used for both trend lines is Bolgokhtokhsk granodiorite (Hawkesworth et al., 1995) with ticks on trend lines representing 2%, 4%, 8% and 12% assimilation. Data sources as in Fig. 6.

compared to Permyakovskaya samples from deeper borehole levels (3.0–4.8 wt.%). This implies that lava flows close to the overlying Triassic sedimentary cover experienced a higher degree of alteration.

Element mobility may account for some of the scatter in Figs. 3 and 4, even for those samples with low LOI. SG-6 sample 96-3 displays low SiO_2 of 45.5 wt.% with high Al_2O_3, $Fe_2O_{3(tot)}$, TiO_2 and MnO, implying the presence of chlorite. In general, the samples from the area of the Khudosey rift show high Al_2O_3 and low MgO in comparison to Urengoy rift samples (Fig. 3e). This may be related to alteration or, more likely, reflect olivine and pyroxene fractionation. The majority of samples are plagioclase-phyric, which may account for the elevated Al_2O_3 concentrations. Correlations between some trace elements (e.g., Ni, Cr, Nb, V, Y and Ba) and MgO (Fig. 4) are consistent with low-pressure fractionation of olivine, plagioclase and clinopyroxene, although the scatter in Rb and Sr is probably related to alteration (Fig. 6a). The range in Cu (16–100 ppm) may reflect the high mobility of this element during hydrothermal alteration although the least altered sample (95-35) displays the lowest concentration (16 ppm). This suggests that the variation in Cu is not exclusively related to alteration but may reflect the influence of sulphide separation, which will be considered later on. Trace elements such as Zr, Ni, V and Nb are least affected by alteration and elevated Ba is correlated with low LOI in sample 95-58 (Table 2).

As mentioned above, samples 97-71 and 95-35 have high Mg#, indicating relatively primitive magma compositions. Bahilovskaya sample 97-71 is, in comparison with other Khudosey rift basalts, elevated in MgO (9.98 wt.%) and Ni (153 ppm) but displays similar high values to several samples from the Urengoy rift (e.g., Yaraynerskaya). Ni contents between 130 and 200 ppm can be derived by 15% fractional crystallisation of olivine from a mantle-derived primitive magma with 300–450 ppm Ni (Allègre et al., 1976). Alternatively, these concentrations may be derived from a less primitive magma, which subsequently accumulated olivine, although we note that sample 97-71 does not contain olivine phenocrysts.

Variation in Ni/V versus Zr (Fig. 8) is controlled principally by olivine, magnetite and pyroxene. To illustrate the effects of these phases, we have carried out simple modelling of Bahilovskaya sample 97-71, which has high Ni, Cr and Mg number consistent with its primitive composition (Fig. 8 inset). During removal of either olivine or magnetite, the Ni/V decreases, whereas during pyroxene removal, Ni/V changes only slightly. Plagioclase fractionation has no

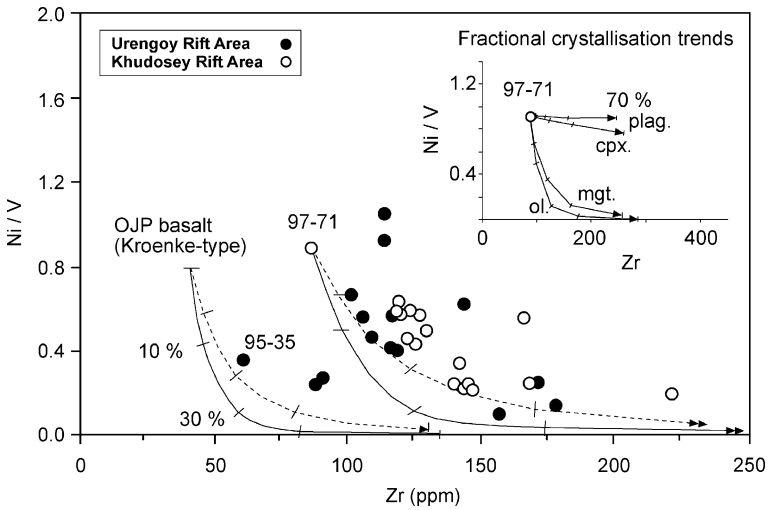

Fig. 8. Variation in Ni/V versus Zr (ppm) indicating history of olivine, magnetite, pyroxene and plagioclase fractionation (inset). Fractionation of olivine (solid line) as well as combined olivine, clinopyroxene and plagioclase (dashed line with modal proportions of 20:30:50, respectively) are illustrated using primitive WSB sample 97-71 and averaged OJP basalt (Kroenke-type) data (Fitton and Godard, 2004). Ticks on crystal fractionation lines represent 10%, 30%, 50% and 70% increments.

effect on Ni/V and increases the concentrations of Ni, V and Zr in the melt. Variations in the fractionating assemblage, from olivine, magnetite to pyroxene and plagioclase, may therefore be identified. The WSB basalts show a large variation in Ni/V (0.4–1.1) within the narrow Zr range of 100–130 ppm, which can be partly ascribed to 10–30% olivine fractionation (Fig. 8). The WSB basalt data can be modelled by olivine fractionation using OJP Kroenke-type or primitive WSB magma. However, slightly smoother trends, fitting the data better, are obtained during combined fractionation of olivine, pyroxene and plagioclase in proportions of 20:30:50 (Fig. 8). It is apparent from Fig. 8 (inset) that marked changes in Ni/V are most likely obtained by olivine (and, possibly, some magnetite) fractionation. Magnetite fractionation may be responsible for the marked difference in Ti/Zr compared to OIB (Kilauea) or N-MORB (Fig. 7). Samples with Zr>130 ppm are from shallower borehole levels and display a smaller range in Ni/V (0.1–0.4), demonstrating a possible change in the fractionation assemblage to pyroxene and plagioclase.

In Fig. 8, sample 95-35 is shifted towards low Ni/V at Zr of 62 ppm. Olivine fractionation alone cannot explain this shift with MgO of 11.6 wt.%, Ni of 44 ppm and the low-Zr content for this sample. The low Ni/V corresponds with low Cu (16 ppm) and may therefore reflect sulphide separation, which is also supported by low Cu/Zr (0.27). Sulphide separation is also implied for the formation of the large Cu–Ni–PGE ore deposits at Noril'sk (Lightfoot et al., 1990, 1993; Naldrett et al., 1992; Fedorenko et al., 1996).

6.2. Comparison between the WSB and the Siberian Traps Noril'sk basalts

The basalts recovered from the WSB are at least in part contemporaneous with the Siberian Traps (Reichow et al., 2002). The Traps crop out in four broad regions, mostly on the Siberian Craton (Zolotukhin and Al'Mukhamedov, 1988; Sharma et al., 1991): Noril'sk, Putorana, Maymecha-Kotuy and Nizhnaya Tunguska (Fig. 1). Noril'sk represents the westernmost part of the Siberian Traps region and is (due to the occurrence of rich Cu–Ni–PGE sulphide deposits) the most extensively studied. Numerous publications (e.g., Naldrett et al., 1992; Lightfoot et al., 1993; Wooden et al., 1993; Hawkesworth et al., 1995; Fedorenko et al., 1996) focus on the basalt sequence at Noril'sk and give detailed geochemical characterisations. (For a detailed review on many of the published data on the Siberian Traps, see Sharma, 1997.) The main chemical characteristics of the different basalt suites in the Noril'sk region are listed in Table 3. Lightfoot et al. (1993) divided the lavas into a lower and upper sequence with high and low TiO_2, respectively. The high-Ti sequence includes the alkaline Ivakinsky, and the subalkaline Syverminsky and Gudchikhinsky suites. Overlying these is the low-Ti sequence comprising eight different suites, which are further divided by Fedorenko (1981) into two assemblages. The first low-Ti assemblage comprises mainly rocks of the Tuklonsky and Nadezhdinsky suites, which precede the main pulse of Siberian Traps. Basaltic tuffs of the Khakanchansky suite form part of this assemblage but limited data availability (only one reported sample) means that they are not considered in this paper. The second low-Ti assemblage, i.e, the main pulse of the Siberian Traps volcanism, comprises five suites of mainly tholeiitic basalts with very uniform major and trace element composition (Table 3), and is therefore treated as one (Upper Series) in this paper.

Several models have been proposed to explain the formation of the Siberian Traps in the Noril'sk region. Few workers dispute the involvement of a mantle plume, although its origin (from the lower or upper mantle) is not clear. Regional uplift should have occurred prior to the onset of this voluminous volcanic activity. Evidence for regional uplift is lacking in the accessible sedimentary cover beneath the Siberian Traps basalts (Czamanske et al., 1998), but Saunders et al. (2005) argue that the main locus of uplift during Permo–Triassic times was located in the WSB, rather than on the Siberian Craton.

The high-Ti basalts show chemical characteristics of deeper-derived melts controlled by garnet, which has been attributed to the direct involvement of a mantle plume (Lightfoot et al., 1993; Wooden et al., 1993). For the generation of the low-Ti basalts, several models have been proposed, including partial melting of the mantle lithosphere (Lightfoot et al., 1990, 1993; Hawkesworth et al., 1995) caused by the heat from the mantle plume or melting of different source regions within the upper (MORB-like) mantle

Table 3
Ranges of selected element abundances and ratios from the Siberian Traps Noril'sk region, Russia[a]. Values in brackets are averages

	Lower sequence (high-Ti)			Upper sequence (low-Ti)						
	Bottom of sequence			First assemblage		Second assemblage (Upper Series)				*Top of sequence*
Suite	Ivakynsky	Syverminsky	Gudchikhinsky	Tuklonsky	Nadezhdinsky	Morongovsky	Mokulaevsky	Kharaelakhsky	Kumingsky	Samoedsky
Abbreviation	Iv	Sv	Gd	Tk	Nd	Mr	Mk	Hr	Km	Sm
SiO_2 (wt.%)	46.2–54.5	49.6–54.7	46.4–52.4	46.8–51.9	49.4–53.5	43.4–50.1	47.7–49.9	48.4–54.9	48.2–48.4	48.4–49.9
	[50.6]	[52.6]	[49.5]	[49.5]	[52.0]	[49.4]	[48.9]	[49.9]	[49.1]	[48.8]
TiO_2 (wt.%)	2.07–3.89	1.46–2.14	1.21–2.37	0.39–0.95	0.83–1.18	0.84–1.27	1.11–1.45	1.31–2.31	1.31–1.52	1.36–1.66
	[2.75]	[1.71]	[1.66]	[0.79]	[0.99]	[1.10]	[1.24]	[1.58]	[1.48]	[1.44]
Mg#[b]	31.6–49.7	54.2–61.3	52.5–74.9	63.6–82.7	53.0–64.4	55.4–61.7	53.0–58.3	39.4–58.9	51.6–55.1	49.5–59.1
	[38.8]	[56.7]	[66.5]	[71.0]	[58.2]	[57.2]	[55.3]	[52.3]	[53.3]	[55.0]
Ni (ppm)	6.0–60	41–111	42–1031	87–383	12–108	51–113	80–155	24–176	87–119	97–146
	[33]	[62]	[486]	[209]	[46]	[107]	[115]	[104]	[100]	[119]
Cu (ppm)	18–48	28–39	21–153	44–127	9.0–135	81–154	64–215	19–215	111–170	107–236
	[31]	[34]	[92]	[80]	[62]	[110]	[141]	[144]	[148]	[169]
Nb/Zr	0.08–0.12	0.07–0.09	0.05–0.23	0.04–0.19	0.04–0.11	0.05–0.06	0.04–0.12	0.04–0.13	0.04–0.09	0.04–0.09
	[0.10]	[0.08]	[0.11]	[0.10]	[0.08]	[0.06]	[0.07]	[0.06]	[0.06]	[0.05]
Ti/Zr	36–62	45–60	56–121	63–93	42–66	48–83	62–92	43–86	69–78	71–87
	[48]	[51]	[96]	[81]	[48]	[69]	[77]	[72]	[72]	[77]
$La/Yb_{(BSE)}$[b]	6.84–9.23	5.4–7.33	3.08–7.31	1.88–2.84	3.23–5.71	1.84–3.38	1.90–3.32	1.42–2.49	2.00–2.16	1.87–2.38
	[7.83]	[6.53]	[3.81]	[2.46]	[4.96]	[2.56]	[2.10]	[1.76]	[2.1]	[1.98]
$La/Sm_{(C1)}$[b]	2.31–3.42	1.97–2.92	1.13–2.36	1.36–1.72	2.06–2.89	1.39–2.51	1.04–1.88	1.13–2.06	1.36–1.56	1.25–1.69
	[2.77]	[2.53]	[1.43]	[1.56]	[2.62]	[1.72]	[1.40]	[1.40]	[1.47]	[1.37]

[a] Data sources: Lightfoot et al. (1990, 1993), Wooden et al. (1993) and Hawkesworth et al. (1995).

[b] BSE and C1 denotes normalisation to bulk silicate earth and chondrite, respectively (McDonough and Sun, 1995). Mg# is calculated as [100×(MgO/FeO+MgO)] assuming Fe_2O_3/FeO of 0.15.

(Fedorenko et al., 1996). However, discrete melting of an asthenospheric mantle plume at various depths with large-scale modification of the magmas at shallow crustal levels was suggested by others (Arndt et al., 1993; Wooden et al., 1993).

Multi-element diagrams for selected WSB samples are compared with averaged data for the Siberian Traps from the Noril'sk area (Fig. 6a and d). Multi-element patterns for the WSB basalts are very similar to the low-Ti Nadezhdinsky suite, suggesting similar conditions of formation. Similar enrichment in LILE and light REE is observed in the high-Ti Ivakinsky (Iv) and Syverminsky suites (Sv). The Iv and Sv suites are, however, clearly lacking the pronounced negative Ti anomalies and display only a minor negative Nb anomaly. These anomalies are far more pronounced in the overlying Nadezhdinsky suite and are attributed to crustal contamination (e.g., Arndt et al., 1993; Wooden et al., 1993) or melting of the lithospheric mantle (Lightfoot et al., 1993; Hawkesworth et al., 1995). In addition, the Siberian Traps basalts have low-Mg numbers, similar to the majority of the WSB basalts, which indicates that neither represents primary magma compositions. Most mantle-derived magmas have therefore been modified en route to the surface, probably in crustal magma chambers.

6.3. Crustal contamination

Fractional crystallisation has controlled some of the chemical variation of the WSB and the Siberian Traps basalts (Section 6.1). However, distinctive features of the WSB basalts include high La/Nb (1–5), high La/Ti and high large ion lithophile element concentrations (e.g., Ba~1300 ppm), combined with low-Ti/Zr ratios (~50) and negative Nb and Ti anomalies (Fig. 6a). These features may be associated with crustal contamination (Cox and Hawkesworth, 1984; Arndt et al., 1993; Wooden et al., 1993).

Incompatible elements such as La or Ba should increase relative to Nb if basaltic magma is contaminated by crustal material, which usually has high La/Nb, Ba/Nb and low La/Ba (Weaver and Tarney, 1984; Wedepohl, 1995). Fig. 9 displays the variation of La/Nb against La/Ba for the WSB basalts, in comparison with other continental flood basalt provinces and a selection of oceanic basalts. Most WSB basalts have higher La/Nb and lower La/Ba ratios than bulk silicate earth with the exception of three samples. This is also observed in other continental flood basalt provinces (e.g., Paraná, Ferrar) and in the Siberian Nadezhdinsky suite. In contrast, high La/Ba and corresponding low La/Nb are characteristic of the Ontong Java Plateau basalts and ocean island basalts such as Kilauea. The shift towards high La/Nb and low La/Ba could be due to post-magmatic alteration. Ba is, in contrast to La, mobile during alteration and the range in La/Ba in the WSB basalt may therefore partly reflect alteration. This is particularly true for sample 96-3 with La/Ba=0.013 and which probably contains chlorite. Low La/Ba values are observed in most Urengoy rift samples; they are also found in samples with low LOI, and therefore the low La/Ba is unlikely to be solely due to alteration. Alternatively, the high La/Nb and low La/Ba can explained by the contamination of sublithospheric magmas as they ascend through the crust, or by melt generation in the lithospheric mantle. Ontong Java Plateau basalts display a large variation of La/Ba, which may be related to seawater alteration and almost uniform La/Nb.

Lightfoot et al. (1993) and Fedorenko (1994) used the Noril'sk Bolgokhtokhsk granodiorite intrusion with high La (90 ppm), Ba (3847 ppm) and Nb (25 ppm), and low TiO_2 (0.37 wt.%) to demonstrate crustal contamination in the formation of the Siberian Traps. We have replicated this mixing calculation, and can show that only 10% bulk assimilation of a Bolgokhtokhsk-type granodiorite is required to account for the range in the WSB compositions (this assumes that the parental basalt magma was derived from 20% melting of a bulk silicate earth source, at a pressure of 3 GPa; see Section 6.6).

Bulk assimilation of crust is possible, if not likely, during the development of a large igneous province, where large (>1000 km^3) basaltic or picritic magma bodies may develop in the crust, in order to store and then erupt to form the large effusive units that are observed at the surface (e.g., Self et al., 1997). A more sophisticated approach is to consider combined wall-rock assimilation and fractional crystallisation (AFC) (DePaolo, 1981) (Fig. 10). It was demonstrated in Fig. 6b that Kilauea, N-MORB and Ontong Java Plateau basalts share some similarities with the WSB basalts, but none of these provides a good match (e.g., negative Nb and Ti anomalies in the WSB basalts).

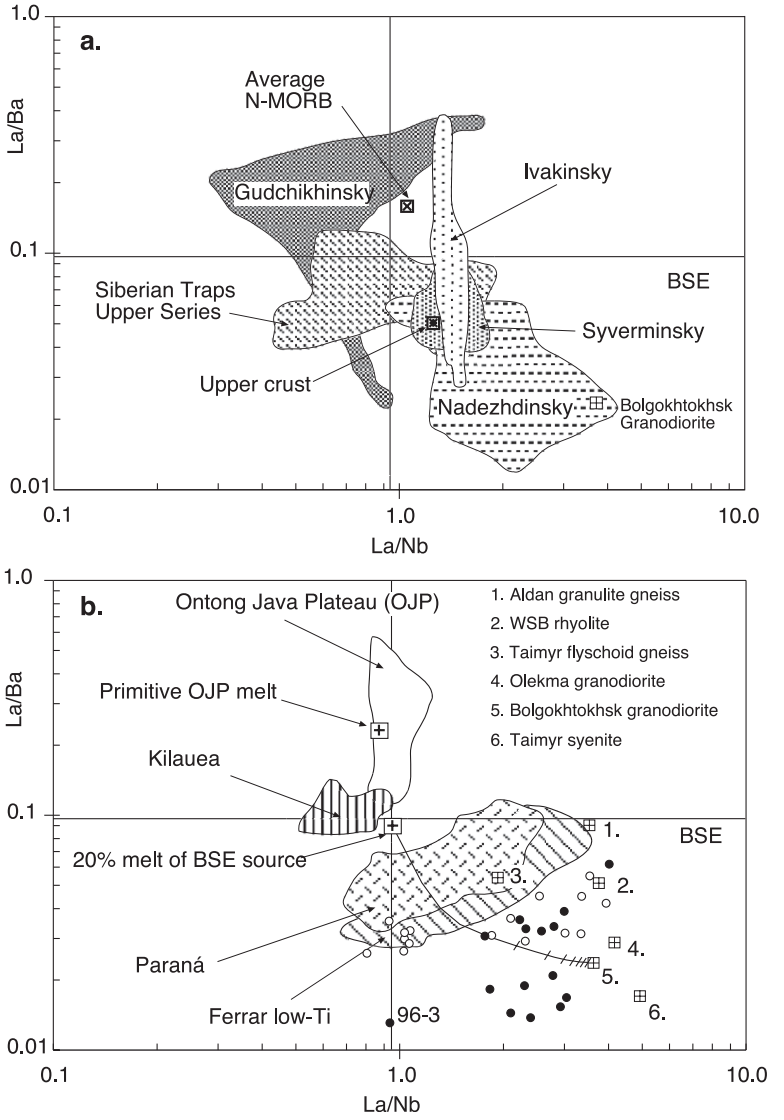

Fig. 9. La/Ba versus La/Nb for the West Siberian Basin basalts compared with various continental flood basalt provinces, ocean island (Kilauea) and MORB. The shift towards high La/Nb and low La/Ba in the WSB (and other) basalts may be explained by contamination of magma by a lower crustal component. Each increment on the simple bulk mixing line represents 10% of assimilated wall rock. Data sources: Ferrar, Kilauea, N-MORB, OJP, Paraná and Siberian Traps as in Fig. 6; Bolgokhtokhsk granodiorite: Hawkesworth et al. (1995); Upper crust: Wedepohl (1995); Aldan Granulite Gneiss and Olekma granodiorite: Jahn et al. (1998); WSB Rhyolite: Medvedev et al. (2003); Taimyr flyschoid gneiss and syenite: Vernikovsky et al. (1995) and Vernikovsky et al. (2003), respectively.

This does not exclude the possibility that the type of magma that was parental to Kilauea, Ontong Java Plateau or N-MORB may also have been parental to the WSB suites, if the latter were subsequently modified by crustal assimilation. In the AFC model calculations, therefore, three parental magmas were used: a primitive magma derived by 20% partial melting of a bulk silicate earth source at 3 GPa, the primitive Ontong Java Plateau magma suggested by Fitton and Godard (2004) and N-MORB (the differences between these are shown on Fig. 11 and in Table 4). Data on basement rocks for the WSB are not available, but the AFC model was tested using basement rocks from the surrounding areas, and a

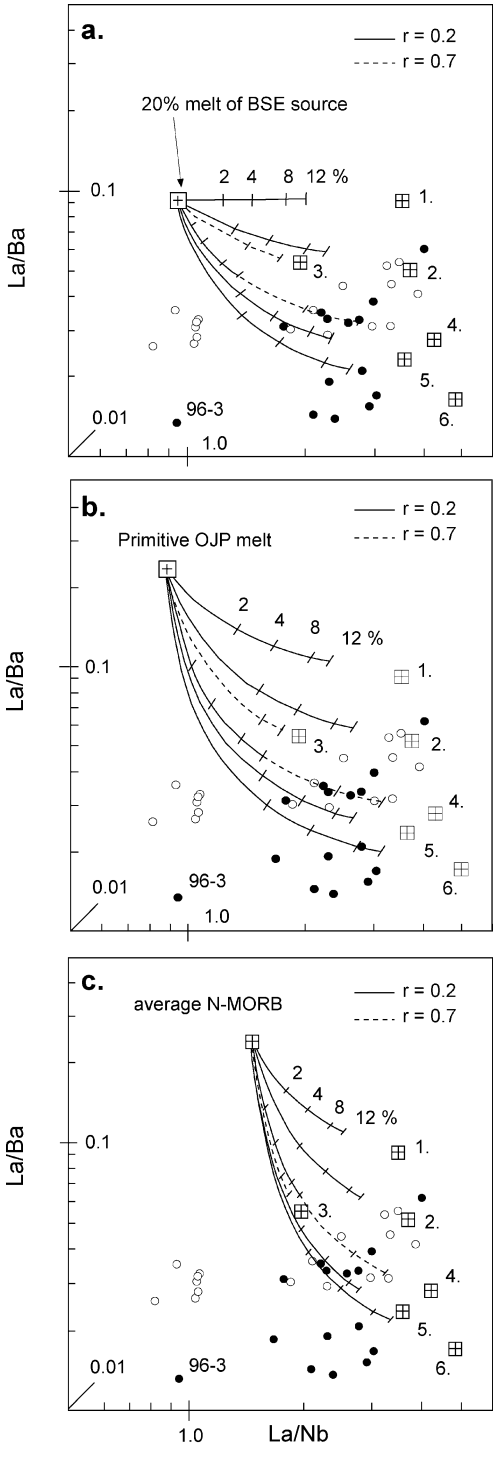

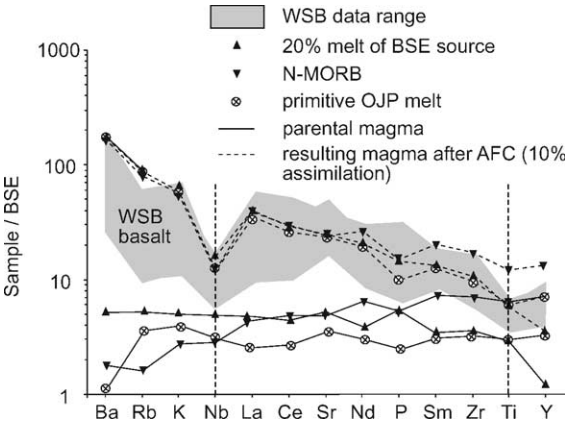

Fig. 11. Multi-element diagram showing WSB basalt range and pattern of magma derived by 20% melting of BSE, primitive OJP melt as suggested by Fitton and Godard (2004) and averaged N-MORB. Dashed lines with symbols represent the three magmas after combined assimilation and fractionation (AFC process) with 10% Taimyr syenite.

WSB rhyolite. The modelled contaminants are, therefore: the Bolgokhtokhsk granodiorite (Hawkesworth et al., 1995), north Taimyr flyschoid gneiss (Vernikovsky et al., 1995), Aldan granulite gneiss, south Siberian Olekma granodiorite (Jahn et al., 1998), WSB rhyolite (Medvedev et al., 2003) and Taimyr syenite (Vernikovsky et al., 2003). As indicated earlier, the low-pressure fractionation assemblage of plagioclase, clinopyroxene and olivine may have dominated the evolution of the WSB basalts. The modal compositions of the fractionating phase in the AFC model are therefore set to 50% for plagioclase, 30% for pyroxene and 20% for olivine. The rate of assimilation in the calculations is assumed to be small (r=0.2) to avoid significant TiO_2 and SiO_2 enrichment.

It is apparent that a primitive magma from a bulk silicate earth source, or the Ontong Java Plateau-type

Fig. 10. AFC model calculations (DePaolo, 1981) for La/Ba and La/Nb for the WSB basalts. The fractionation assemblage is plagioclase, clinopyroxene and olivine in modal abundances of 50:30:20. Parental magmas are: (a) 20% melt of BSE source, (b) primitive OJP melt and (c) average N-MORB. Contaminants are as in Fig. 9 and assimilation to fractionation rates (M_a/M_c=r) are shown for r=0.2 (solid line) and 0.7 (dashed line, shown only for Taimyr flyschoid gneiss and Olekma granodiorite). Increments on AFC trend lines for r=0.2 correspond to 2%, 4%, 8% and 12%, whereas for r=0.7 only 21% and 45% are shown. Values and model parameters used are given in Table 4.

Table 4
Results and parameters for the AFC model calculations

	Ba	Rb	K	Nb	La	Ce	Sr	Nd	P	Sm	Zr	Ti	Y
Contaminant													
Taimyr syenite[a]	4561	194	50103	15.9	79.2	136	2244	68.9	2095	11.5	167	3657	25.3
Bolgokhtokhsk[b]	3847	147	42921	25.0	90.3	178	1640	64.2	1426	9.3	253	2218	15.3
Parental magmas													
Primitive OJP[c]	7.14	2.1	925	1.91	1.66	4.48	70.8	3.82	224	1.25	33.7	3645	14
$BSE_{20\%}$[d]	33.6	3.07	1220	3.23	3.04	7.41	102	4.69	460	1.37	38.1	3414	5.1
Average N-MORB[e]	12.03	0.96	664	1.96	2.9	8.29	97.3	8.21	480	2.89	76.4	7734	29.7
Results for AFC model (II) using Taimyr syenite as contaminant and with modal abundance of fractionating phases: plagioclase (50%), clinopyroxene (30%), olivine (20%), magnetite (0%); values after 10% assimilation and 40% fractional crystallisation, rate of assimilation to fractionation: r=0.2													
Primitive OJP	1099	51.5	14284	7.8	22.7	42.3	455	23.8	878	5.0	103	7318	30.6
$BSE_{20\%}$	1151	53.4	14868	10.4	25.3	48.0	485	25.5	1291	5.3	111	6908	14.9
Average N-MORB	1112	49.3	13768	7.9	25.1	49.7	481	32.1	1326	8.1	182	14,567	58.2
Results for AFC model (II) using Bolgokhtokhsk granodiorite as contaminant and with modal abundance of fractionating phases: plagioclase (50%), clinopyroxene (30%), olivine (20%), magnetite (0%), values after 10% assimilation and 40% fractional crystallisation, rate of assimilation to fractionation: r=0.2													
Primitive OJP	928	40.0	12499	10.0	25.4	52.6	351	22.7	723	4.5	124	6981	28.3
$BSE_{20\%}$	981	41.9	13083	12.7	28.1	58.3	382	24.3	1135	4.7	132	6572	12.6
Average N-MORB	941	37.8	11982	10.1	27.8	60.0	377	31.0	1170	7.5	203	14,231	55.9
D_{values} *(taken from compilation given in Bédard, 1994)*													
Ol	0.0005	0.0005	0.0068	0.0100	0.0004	0.0003	0.0160	0.0002	0.019	0.0002	0.0030	0.0070	0.0020
Cpx	0.00068	0.011	0.0072	0.0077	0.0536	0.0858	0.1283	0.1873	0.0044	0.2910	0.1234	0.3840	0.4670
Plag	0.18966	0.08	0.017	0.0010	0.0420	0.0360	1.5593	0.0290	0.01	0.0220	0.0900	0.0450	0.0100
mgt	0.028	0.32	0.045	0.0100	0.0006	0.0006	0.0005	0.0006	0.01	0.0006	0.0400	16.5	0.0039

[a] Vernikovsky et al. (2003).
[b] Hawkesworth et al. (1995).
[c] Fitton and Godard (2004).
[d] McDonough and Sun (1995).
[e] Salters and Stracke (2004).

parental magma, requires only 4 to 12% assimilated Taimyr syenite or Bolgokhtokhsk granodiorite wall-rock to account for most of the compositional range observed in the WSB basalts (Fig. 10 and Table 4). The Olekma granodiorite from south Siberia has similar La/Ba and La/Nb ratios to the Bolgokhtokhsk granodiorite, but has much lower abundances of these elements necessitating an increase of assimilation to 21–42% (r=0.7, Fig. 10) to account for the observed compositional range. Higher rates of assimilation would be expected at the high temperatures at lower crustal levels, or diffusing from a large and hot basalt magma body. However, La/Ba ratios <0.03 require contaminants with Ba concentrations much higher than in the Olekma granodiorite. High rates of assimilation of low-Ba contaminants therefore cannot explain the observed ratios. Furthermore, higher rates of assimilation would also increase the amount of assimilated SiO_2 and TiO_2, but samples close to the Olekma AFC model line with r=0.7 are not particularly elevated in either. The AFC model calculations also show that neither the Aldan granulite nor Taimyr flyschoid gneiss can account for the data, even at high rates of assimilation (Fig. 10, shown only for the latter).

The calculations were re-run using a parental magma with N-MORB composition (i.e., with lower abundances of La, Ba, Nb than in the 20% melt from a bulk silicate earth source). Assimilation of 2–12% of Taimyr syenite or Bolgokhtokhsk granodiorite account for some of the WSB basalt data but samples with low La/Ba and La/Nb cannot be reproduced.

Contamination of N-MORB magma by Taimyr flyschoid gneiss or Aldan granulite cannot account for the range of WSB basalt data, even at high rates of assimilation. Similarly, the elevated La/Ba (>0.04) and La/Nb (>3.0) are probably not produced by the addition of silicic crust similar to WSB rhyolite or Aldan granulite gneiss to either of the three parental magmas used here, as the WSB data does not plot along these trend-lines.

To summarise, the AFC modelling described above can account for the low La/Ba and high La/Nb of many of the WSB (and Nadezhdinsky) basalts. The data are consistent with contamination of a parental magma by a crustal rock similar in composition to the Taimyr syenite or the Bolgokhtokhsk granodiorite. The composition of the parental magma, whilst not tightly constrained, may be similar to the parental melt of the Ontong Java Plateau, or a 20%, 3 GPa melt from bulk silicate earth, as these accommodate the WSB data best. Nonetheless, the described assimilation fails to reproduce the very low La/Ba (<0.02) found in some of the WSB basalts. At least two explanations could account for this discrepancy: post-magmatic alteration and/or assimilation of crustal rocks with very low La/Ba.

6.4. Origin of the low-Ti signature

In the previous sections, we demonstrated that the magma parental to the WSB basalts was modified by olivine, plagioclase and pyroxene fractionation, and subsequently contaminated by continental crust. The bulk of the analysed basalts from the WSB, and the Nadezhdinsky suite, all have low Ti/Zr (~50) when compared with oceanic basalts and many continental flood basalts (Fig. 7). This observation, plus several others highlighted elsewhere in this paper, effectively rules out *direct* derivation of the WSB basalts from a parental magma resembling N-MORB (Ti/Zr~100–120), primitive OJP basalt (Ti/Zr~110) or a melt from a bulk silicate earth source (Ti/Zr~90). This low-Ti characteristic has been identified in many other continental flood basalt provinces, including Ferrar (Hergt et al., 1991), Paraná (Peate and Hawkesworth, 1996) and Madagascar (Storey et al., 1997). Its origin has been attributed to crustal assimilation (Arndt et al., 1993) or source composition (Hergt et al., 1991; Brewer et al., 1992); the latter is particularly important, because it has led to suggestions that low-Ti tholeiites may be derived from the continental lithospheric mantle (Hergt et al., 1991), with all the implications for the generation of flood basalts that ensue.

It is possible to generate the low-Ti/Zr ratios seen in the WSB basalts using our preferred model discussed in Section 6.3 (i.e., contamination of OJP or bulk silicate earth magma by 12% of Bolgokhtokhsk granodiorite or Taimyr syenite rock) (line ‘a’ on Fig. 7). If the contaminant has a similar Ti concentration to the Taimyr syenite, small amounts (1–2%) of magnetite included in the fractionating assemblage are required. Ariskin and Barmina (1999) show that magnetite fractionation is strongly dependent on the oxygen fugacity of the melt. Both the oxygen and silica activities may be significantly changed during the AFC process, thus enhancing magnetite stability and modifying the partitioning of Ti into magnetite. This may lead to enhanced removal of both Fe and Ti from the melt. If this suggestion is correct, then it precludes the necessity of melting the lithospheric mantle to produce low-Ti tholeiites.

6.5. Nature of the parental melts and the mantle source

The difference between N-MORB, OIB (Kilauea) and the WSB basalts becomes clear when using a plot of Nb versus Zr (Fig. 5). The majority of the WSB data plot with a near constant value of Nb/Zr (0.055), between OIB and N-MORB, but similar to OJP basalts (Fitton and Godard, 2004). Zr and Nb are least affected by alteration, and are incompatible during fractional crystallisation of olivine, pyroxene, magnetite and plagioclase from a basaltic magma, and thus provide an indication of the composition of the parental if not primary magmas. These (and other) data indicate that the parental magma of the WSB basalts more closely resembles that which produced the OJP basalts, rather than N-MORB or ocean island basalts such as Kilauea. Some basalts from lower sections of the Permyakovskaya borehole are elevated in Nb (and Nb/Zr) compared to the rest of the WSB basalts, and plot in the OIB (Kilauea) field. This high-Nb/Zr ratio cannot be explained solely by AFC processes as putative contaminants have generally lower or similar Nb/Zr to the other WSB tholeiites,

suggesting that the parental melts inherited high Nb/Zr either from the source, or during the melting event. It is apparent from Fig. 5 that the majority of the WSB basalts may ultimately be derived from a parental melt similar to that, which supplied the OJP. Fitton and Godard (2004) argue that this parental OJP melt was derived by large degrees of melting (~27–30%) of a primitive mantle source originally depleted by extraction of 1% by mass of average continental crust. The timing of this original extraction event was probably in the Archaean (Tejada et al., 2004), but the point that concerns us here is to estimate the likely composition of the source mantle—namely, slightly depleted in highly incompatible elements, with near-chondritic REE profiles and Nb/Zr ratios.

Trace element data are sensitive to the effects of partial melting and can be used to constrain the pressure and extent of melting. REE such as La, Gd and Yb are particularly useful, because their relative abundances are strongly dependent on the degree of partial melting and the nature of the aluminous phase (spinel or garnet) in the mantle source. The WSB basalt data form a positive array on a diagram of La/Yb versus Gd/Yb (Fig. 12). The $Gd/Yb_{(BSE)}$ ratio in the WSB basalts varies only slightly (0.9–1.8), whereas $La/Yb_{(BSE)}$ displays much higher variation (1.8–8.8). In comparison, similarly large variations in $La/Yb_{(BSE)}$ for the Siberian Traps basalts are observed in the Nadezhdinsky suite (Wooden et al., 1993). The WSB basalts have similar or lower $Gd/Yb_{(BSE)}$ ratios of 1.7 compared to the Siberian Traps low-Ti basalts, whereas the Noril'sk high-Ti basalts (Ivakinsky, Syverminsky, Gudchikhinsky) display $Gd/Yb_{(BSE)}$ ratios >1.7 (Fig. 12). The only exception to this is Hohryakovskaya sample 97-97 with $Gd/Yb_{(BSE)}$=1.86 similar to ratios of the Ivakinsky suite. N-MORB and OJP basalts display, in contrast to the WSB basalts, much lower La/Yb and Gd/Yb ratios.

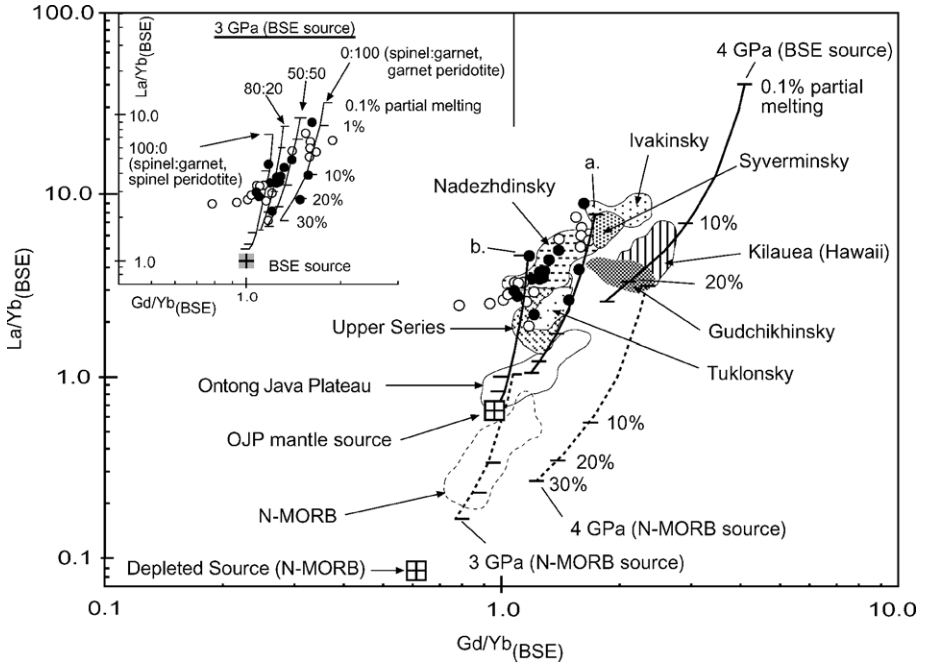

Fig. 12. La/Yb versus Gd/Yb (normalised to bulk silicate earth: McDonough and Sun, 1995) displaying the range of REE in the WSB basalts and possible correlation with partial melting. Data from Kilauea, N-MORB (for clarity only indicated by dashed line), Ontong Java Plateau and the Siberian Traps are also shown for comparison (data sources as in Fig. 6). Trend lines are calculated for an OJP mantle, initial BSE and depleted (N-MORB) mantle source assuming non-modal batch melting. Bulk distribution coefficients are calculated using mineral proportions for garnet peridotite at 3 and 4 GPa after Walter (1998) and spinel peridotite given by McKenzie and O'Nions (1991). Melting of the OJP mantle source for garnet peridotite and spinel peridotite at 3 GPa is indicated by trend line (a) and (b), respectively. Partial melting within the garnet-spinel transition zone at 3 GPa is modelled for the initial BSE source (inset). Distribution coefficients used for the REE are from Hanson (1980) and Hart and Dunn (1993).

Large variations in La/Yb can be related to changes in the degree of partial melting, fractional crystallisation and to crustal contamination, or a combination of these. As shown above, La was probably increased in the WSB basalts by crustal contamination, which is indicated by elevated La/Yb combined with high SiO_2 for some of the basalts. Melts derived by partial melting within the garnet stability field display both high-Gd/Yb and -La/Yb ratios, because garnet preferentially retains the heavy REE relative to the light and middle REE. Data from Kilauea, Hawaii (Chen et al., 1996; Norman and Garcia, 1999) in Fig. 12 represent basalts derived by small degrees of partial melting within the garnet stability field. N-MORB and basalts from the OJP are, in contrast, derived by larger degrees of melting at shallower mantle levels. It is apparent from Fig. 12 that the Siberian Traps lower suites (Ivakinsky, Syverminsky and Gudchikhinsky) are likely to be derived from a deep source and probably by small degrees of partial melting in the garnet stability field (e.g., Wooden et al., 1993), similar to Hawaii. Basalts from stratigraphically higher suites (including the Tuklonsky and Nadezhdinsky suites) are, in contrast, likely to represent higher degrees of melting at shallower levels (Sharma, 1997).

6.6. Partial melting model

Simple modelling can illustrate the depth and degree of melting necessary to account for the variation in REE ratios of the WSB, and helps to constrain whether spinel or garnet was present in the source. The model parameters are set assuming the melt generation is by non-modal batch melting, rather than fractional melting, and several scenarios are illustrated:

1. Melting of garnet and spinel peridotite with OJP mantle source composition (primitive mantle after depletion of 1% melt as suggested by Fitton and Godard, 2004) at 3 GPa (Fig. 12, lines a and b, respectively).
2. Melting of garnet peridotite with depleted mantle composition (N-MORB source) at pressures of 3 and 4 GPa (Fig. 12, dotted lines).
3. Melting of garnet peridotite with primitive mantle (BSE) composition at 4 GPa (Fig. 12).
4. Melting of mantle peridotite containing spinel and garnet in different proportions and with primitive mantle (BSE) composition at 3 GPa (Fig. 12, inset).

Melts parental to the WSB basalts were contaminated by continental crust, which has a strong influence on the La/Yb ratio but minor effects on Gd/Yb. Therefore, the model can only be regarded as semi-quantitative and used for guidelines only. Nevertheless, the partial melting model may still be of use to identify the most likely source and degree of melting responsible for the generation of the WSB basalts.

Bulk distribution coefficients (D_{Bulk}) are calculated using mineral proportions for garnet peridotite at 3 and 4 GPa after Walter (1998) and for spinel peridotite after McKenzie and O'Nions (1991). Mineral-melt distribution coefficients for the REE are taken from Hanson (1980) with the exception of pyroxene, which are taken from Hart and Dunn (1993). D_{Bulk} values are a function of source composition, pressure and temperature, but for simplicity are assumed to be constant over the calculated melting regime. The relative mineral proportions entering the melt predict that clinopyroxene and garnet are exhausted after 25% melting, leaving a harzburgite residue. The validity of the calculation for the WSB basalts is constrained by modelling data from Kilauea and the Siberian Gudchikhinsky suite. According to the calculations, 10–20% partial melting of garnet peridotite with initial BSE composition at a pressure of 4 GPa is required to obtain the Kilauea and Gudchikhinsky data (Fig. 12). This corresponds well to depth (>100 km) and degree of melting (5–15%) estimates for the generation of the Kilauea magmas (Watson and McKenzie, 1991; Norman and Garcia, 1999), and the proposed garnet-bearing source for the Siberian Gudchikhinsky suite (Wooden et al., 1993).

Trends shown in Fig. 12 reflect the differences in the degree of melting in relation to the Al-bearing phase in the source region. The WSB data lie within the modelled partial melting trends defined by spinel and garnet peridotite with OJP source composition at 3 GPa and degrees of melting <10%. It is apparent from Fig. 12 (inset) that partial melting of spinel and garnet peridotite with an initial BSE composition can account for most of the WSB data. Robinson and

Wood (1998) report that the garnet-spinel transition occurs at pressures between 3.1 and 2.8 GPa, which would suggest generation for the WSB basalt magmas at depths shallower than 100 km. Calculating partial melting of mantle peridotite in the garnet-spinel transition zone with increasing proportions of spinel clearly illustrates this possibility. The degrees of melting required to match most of the WSB data are in the range of 1–20% with increasing proportions of spinel.

Although it seems reasonable that melting occurred within the garnet-spinel transition zone or close to the spinel stability field, the $La/Yb_{(BSE)}$ ratios >5 seen in the WSB basalts can only be explained by very small degrees of partial melting (<<1%), which are too small to be reasonable. The composition of the source for the WSB basalts is poorly constrained and might be heterogeneous or more enriched than that assumed for the modelling. This fact, together with the reliability of distribution coefficients, has strong implications for the model calculations. Alternatively, and as discussed above, the concentration of La, being substantially higher in crustal rocks (with $La/Yb_{(BSE)}$ ratios >5) may be the result of crustal contamination rather than reflecting various degrees of partial melting of a homogeneous mantle source. The WSB basalts display a similar large variation in La/Yb to the Nadezhdinsky suite, for which crustal contamination is implied (Lightfoot et al., 1993; Wooden et al., 1993). Several high-$La/Yb_{(BSE)}$ WSB basalts are elevated in SiO_2 (~51 wt.%), which would be expected if the magma were contaminated by crustal lithologies. It is clear that melting of an OJP source or depleted (N-MORB) source alone cannot account for the observed data range, and addition of incompatible elements is required. The AFC model calculations in Section 6.3 demonstrate that melts derived from the three supposed sources contaminated by continental crust can account for some of the WSB data. Initial melts derived from a depleted (N-MORB) source have much lower La/Yb in comparison to those derived from an OJP-type source at similar degrees of melting (Fig. 12). This consequently requires higher amounts of assimilation by melts derived from a depleted source to increase La/Yb to the WSB basalt ratios, compared to melts derived from an OJP-type source.

6.7. Melting of the mantle lithosphere

Hergt et al. (1991) argue that to account for the pronounced negative Nb and Ti anomalies observed in some continental flood basalt provinces, unrealistically large amounts of assimilated crust, or unrealistically depleted parental magmas, are required. An alternative model to crustal contamination is melting of the sublithospheric mantle. The bulk of the lithospheric mantle (i.e., that above the thermal boundary layer) is substantially cooler than the underlying convective mantle. It therefore requires additional heat to induce melting (McKenzie and Bickle, 1988). An underlying plume may supply the additional heat required to melt the anhydrous lithosphere, but the melt volume produced is insufficient to account for the volume observed in continental flood basalt provinces (Arndt and Christensen, 1992). Partial melting of a hydrous mantle lithosphere, which is trace-element enriched due to previous subduction events, is therefore favoured by some authors (Hergt et al., 1991; Turner and Hawkesworth, 1995; Hawkesworth et al., 2000). This source could contain the low Ti, Nb and elevated LILE concentrations observed in some CFB suites. Extensive Palaeozoic collision zones influenced the WSB to the south, west and north (Fig. 1), and therefore hydration and subduction-related enrichment of the mantle lithosphere beneath the WSB is possible. Furthermore, the WSB basalts are vesicle-rich, and gabbros contain biotite, suggesting that the magmas may have been volatile-rich. Melts derived from a hydrous source are silicate- and water-rich, but low in CaO, Fe_2O_3 and TiO_2 (Green, 1973). The SiO_2 and water content would subsequently increase during fractional crystallisation. However, both conduction of heat into and extension of the lithosphere are slow processes (at least on the scale of the production of the Siberian large igneous province), and are unable to generate large volumes of melt (2×10^6 km^3) in very short intervals of time (<2 Myr).

6.8. Petrogenesis of the WSB basalts

Any model explaining the generation of the WSB basalts has to take into account their high LILE concentration and their relative depletion in Nb and Ti. As shown above, the WSB basalts show strikingly

similar chemical characteristics to the low-Ti basalts from the Noril'sk succession, in particular the Nadezhdinsky suite. The low-Ti signature of the Nadezhdinsky suite and the WSB basalt may reflect high (and shallow) degrees of melting within a mantle plume. This may account for the absolute low Ti and Nb abundances, but cannot easily account for the varying inter-element ratios.

We have argued above that melting of a primitive (BSE) or an OJP-type mantle source within the garnet-spinel transition zone (<3 GPa) may account for the low-Ti signature of the WSB basalt, and that their high-K,-Ba and -light-REE characteristics are the effect of subsequent crustal assimilation. Although some of the WSB data can be modelled using a source similar to that of N-MORB, the calculations demonstrate that using primitive BSE or OJP sources accommodate the data best (Fig. 10). Furthermore, we argue that higher rates of assimilation are required if the primitive melts were derived from a depleted (N-MORB) source than primitive BSE or OJP-type sources at similar degrees of melting (Fig. 12).

Low Nb, Ti and high light-REE abundances are in some continental large igneous provinces attributed to partial melting of the sub-continental lithospheric mantle (similar to the low-Ti basalts from the Ferrar or Paraná provinces: e.g., Hergt et al., 1991; Hawkesworth et al., 2000). Such melting may have been triggered by a mantle plume or by extension and decompression of the lithosphere. Reichow et al. (2002) demonstrated that the WSB basalts were emplaced around ~250 Ma with an estimated volume of 1.3×10^6 km^3 and probably within less than 2 Myr. Passive rifting of the lithosphere produces only minor volumes of melt and cannot account for the volume observed on such a short timescale (Arndt and Christensen, 1992). Increased melting of the sublithospheric mantle could occur if a hot mantle plume supplies heat or the sublithospheric mantle contains water (Gallagher and Hawkesworth, 1992). Lightfoot et al. (1993) argue for partial melting of the sublithospheric mantle to account for the negative Nb and Ti anomalies in the Siberian basalts. However, Arndt and Christensen (1992) demonstrated that during increased melting of the sublithospheric mantle caused by the heat supply of a mantle plume, the lithospheric mantle signature of the melt would be lost due to the introduction of asthenospheric mantle melt. We therefore consider melting of lithosphere in the case of the WSB basalts as unlikely. The increased LILE and light-REE signature of the WSB basalts can be modelled by small amounts of assimilation of crustal rocks (~12%) by a primitive magma. High assimilation rates are not required if the contaminant is similar to the Taimyr syenite or Bolgokhtokhsk granodiorite, as demonstrated in Section 6.3.

Saunders et al. (2005) argue that late Permian–Triassic rifting in the WSB is possibly caused by the doming effect of an uprising mantle plume. Extension alone could not trigger the observed large-scale volcanic activity on a timescale of less than 2 Myr. The thinned WSB lithosphere may have opened the way for the high degrees of melting required to generate the low-Ti and other basalts (Saunders et al., 2005). The lithosphere beneath the WSB is even today hotter and thinner relative to the adjacent Siberian Craton (Pavlenkova et al., 2002). These primitive melts ascended and interacted with the crust and/or sub-continental lithosphere, giving the observed range of compositions. Fractional crystallisation of predominantly olivine, clinopyroxene and plagioclase, and crustal assimilation of up to 12% can explain the element signatures of the WSB basalts.

The low-Ti Upper Series basalts from Noril'sk are by far the most voluminous of the Siberian basalts, and similar basalts cover vast areas of the Siberian Craton (Sharma et al., 1991, 1992). It is argued (e.g., Sharma et al., 1992; Wooden et al., 1993) that these Upper Series basalts represent the main melting event within the plume, which by this time had risen (via lithospheric thinning) to shallower depths and lower pressures (ca. 2 GPa). Oddly, few Upper Series tholeiites are found in the WSB sequences. This may be a problem of limited sampling, or may be because the lavas were not erupted or preserved in the central and southern regions of the Basin (for a more complete discussion, see Saunders et al., 2005).

The earliest basalts erupted at Noril'sk include the high-Ti and high-Gd/Yb tholeiitic basalts and picrites of the Ivakinsky, Syverminsky and Gudchikhinsky suites. These high-Ti basalts are probably derived by relatively deep (ca. 4 GPa) melting (e.g., Wooden et al., 1993) beneath a moderately thick lithosphere (ca. 100 km) and have undergone only minor contamination during their ascent through the lithosphere.

This type of basalt has not been recovered from the WSB or alternatively, may occur deeper in the boreholes, and has simply not been sampled. It is likely that these deeply sourced basalts originated from hotter-than-ambient mantle (in order for sufficient melting to occur), and thus require the involvement of a mantle plume (Wooden et al., 1993; Sharma et al., 1992). Alternative models, such as 'edge' models (e.g., King and Anderson, 1995, 1998), advocate much smaller increases in mantle potential temperature, and it is difficult to see how sufficient melting could occur at such high pressures. Catastrophic decompression of a hot mantle plume head (Campbell and Griffiths, 1990) remains the best explanation for the voluminous magmatic activity of the WSB and Noril'sk Nadezhdinsky suite basalt.

The large volumes, wide areal extent and the rapid eruption rates of the low-Ti WSB basalts, require a widespread and voluminous source, most probably a mantle plume, which is the most effective carrier of the large amounts of energy and material required for the melting process. Our preferred model in the generation of the WSB basalts is derivation of the primitive magmas by large degrees of melting within the garnet-spinel transition zone or close to the spinel stability field. These melts were contaminated by crustal lithologies similar in composition to the Taimyr syenite or the Bolgokhtokhsk granodiorite. The source composition of the mantle parental to the WSB basalts was probably similar to that of the Ontong Java Plateau basalts, or a 20% melt from bulk silicate earth. Primitive melts derived from this type of source are low in Ti and require a relatively small amount of contaminant, fitting the WSB basalt data best.

7. Conclusions

Major and trace element data of the WSB basalts are typical of fractionated, crustally contaminated continental flood basalts (e.g., low Mg#, and negative Nb and Ti anomalies on mantle-normalised plots). The chemistry of the WSB basalts resembles the Siberian Traps low-Ti Nadezhdinsky suite (Noril'sk region) but also shows some similarities with basalts from the Upper Series from Noril'sk. The observed geochemical variations in the WSB data are consistent with processes involving low-pressure fractionation of plagioclase, clinopyroxene and olivine as the main fractionating phases, and with wallrock assimilation (AFC processes). We argue that the compositions of the WSB basalts can be modelled by large degrees of partial melting (20–30%) and subsequent modification by AFC processes. The composition of the parental magma cannot be tightly constrained but melts parental to the Ontong Java Plateau, or a 20% melt from bulk silicate earth derived at 3 GPa, accommodate the data best when contaminated with continental crust similar to Taimyr syenite or Bolgokhtokhsk granodiorite. The model calculations show that at small rates of assimilation to fractionation (r=0.2) only 6–12% assimilant are required to account for the WSB data.

In some continental large igneous provinces, low Nb, Ti and high light-REE abundances are attributed to partial melting of the sub-continental lithospheric mantle, triggered either by a mantle plume or by extension and decompression of the lithosphere. Volumes of melt produced by passive rifting of the lithosphere cannot account for the volumes of basalt observed in the WSB, in particular on the time scale of <2 Myr. Generation of the WSB basalts due to melting of the sublithospheric mantle (hydrous or anhydrous) is considered as unlikely although a contribution from the sublithospheric mantle cannot be excluded. The geochemical characteristics like low-Ti and Nb abundances are consistent with derivation of the WSB basalts via large scale melting of a mantle plume. Moreover, the magma volume and timing constraints strongly suggest that a mantle plume was involved in the formation of the Earth's largest continental flood basalt province.

Acknowledgments

The authors are grateful to Dr. N.P. Kirda (Institute of Geology, Oil and Gas, SB RAS, Novosibirsk) for providing samples from the West Siberian Basin. An earlier version of this manuscript greatly benefited from reviews by Hilary Downes. Furthermore, we would like to thank Ray W. Kent, Andrew C. Kerr and Lotte M. Larsen for their constructive reviews, which significantly improved the manuscript. These investigations were supported by the Russian Foundation

for Basic Research (grant # 03–0565206). MKR is supported by a University of Leicester Scholarship and RVW is supported by a Royal Society Dorothy Hodgkin Research Fellowship.

References

Afonin, V.P., Gunicheva, T.N., Piskunova, L.F., 1984. XRF Silicate Analysis. Nauka, Novosibirsk, p. 227. In Russian.

Allègre, J.C., Treuil, M., Minster, J.-F., Minster, B., Albarède, F., 1976. Systematic use of trace element in igneous process: Part 1. Fractional crystallisation processes in volcanic suites. Contrib. Mineral. Petrol. 12, 56–75.

Al'Mukhamedov, A.I., Medvedev, A.Ya., Kirda, N.P., 1999. Comparitive analysis of geodynamic settings of the Permo–Triassic magmatism in East Siberia and West Siberia. Russ. Geol. Geophys. 40 (No. 11), 1550–1561.

Anderson, D.L., 1994. The sublithospheric mantle as the source of continental flood basalts; the case against the continental lithosphere and plume head reservoirs. Earth Planet. Sci. Lett. 123, 269–280.

Aplonov, S., 1988. An aborted Triassic ocean in West Siberia. Tectonics 7, 1103–1122.

Aplonov, S.V., 1995. The tectonic evolution of West Siberia; an attempt at a geophysical analysis. Tectonophysics 245, 61–84.

Ariskin, A.A., Barmina, G.S., 1999. An empirical model for the calculation of spinel-melt equilibria in mafic igneous systems at atmospheric pressure: 2. Fe–Ti oxides. Contrib. Mineral. Petrol. 134, 251–263.

Arndt, N.T., Christensen, U., 1992. The role of lithospheric mantle in continental flood volcanism: thermal and geochemical constrains. J. Geophys. Res. 97, 10967–10981.

Arndt, N.T., Czamanske, G.K., Wooden, J.L., Fedorenko, V.A., 1993. Mantle and crustal contributions to continental flood volcanism. Tectonophysics 223, 39–52.

Bédard, J.H., 1994. A procedure for calculating the equilibrium distribution of trace elements among the minerals of cumulate rocks, and the concentration of trace elements in the coexisting liquids. Chem. Geol. 118, 143–153.

Bochkarev, V.S., Brekhuntsov, A.M., Deshchenya, N.P., 2003. The Paleozoic and Triassic evolution of West Siberia (data of comprehensive studies). Russ. Geol. Geophys. 44 (No. 1–2), 120–143.

Brewer, T.S., Hergt, J.M., Hawkesworth, C.J., Rex, D., Storey, B.C., 1992. Coats land dolerites and the generation of Antartic continental flood basalts. In: Storey, B.C., Alabaster, T., Pankhurst, R.J. (Eds.), Magmatism and the Causes of Continental Break-up, vol. 68. Geological Society of London Special Publication, London, pp. 185–208.

Campbell, I.H., Griffiths, R.W., 1990. Implications of mantle plume structure for the evolution of flood basalts. Earth Planet. Sci. Lett. 99, 79–93.

Chen, C.-Y., Frey, F.A., Rhodes, J.M., Easton, R.M., 1996. Temporal geochemical evolution of Kilauea Volcano: comparison of Hilina and Puna basal. In: Basu, A., Hart, S. (Eds.), Earth Processes: Reading the Isotopic Code, vol. 95. American Geophysical Union Monograph, Washington, DC, pp. 161–181.

Cox, K.G., Hawkesworth, C.J., 1984. Relative contributions of crust and mantle to flood basalt magmatism, Mahabaleshwar area, Deccan Traps. Philos. Trans. R. Soc. Lond. A310, 627–641.

Czamanske, G.K., Gurevitch, A.B., Fedorenko, V., Simonov, O., 1998. Demise of the Siberian plume: paleogeographic and paleotectonic reconstruction from the prevolcanic and volcanic record, North–Central Siberia. Int. Geol. Rev. 40, 95–115.

DePaolo, D.J., 1981. Trace element and isotopic effects of combined wallrock assimilation and fractional crystallisation. Earth Planet. Sci. Lett. 53, 189–202.

Fedorenko, V.A., 1981. Petrochemical series of extrusive rocks of the Noril'sk region. Sov. Geol. Geophys. 22 (6), 41–47.

Fedorenko, V.A., 1994. Evolution of magmatism as reflected in the volcanic sequences of the Noril'sk region. In: Lightfoot, P.C., Naldrett, A.J. (Eds.), Proc. Sudbury-Noril'sk Symp., OGS Spec., vol. 5, pp. 171–184.

Fedorenko, V.A., Lightfoot, P.C., Naldrett, A.J., Czamanske, G.K., Hawksworth, C.J., Wooden, J.L., Ebel, D.S., 1996. Petrogenesis of the flood-basalt sequence at Noril'sk, North Central Siberia. Int. Geol. Rev. 38, 99–135.

Fitton, J.G., Godard, M., 2004. Origin and evolution of magmas on the Ontong Java Plateau. In: Fitton, J.G., Mahoney, J.J., Wallace, P.J., Saunders, A.D. (Eds.), Origin and Evolution of the Ontong Java Plateau, vol. 229. Geological Society of London Special Publication, London, pp. 151–178.

Gallagher, K., Hawkesworth, C.J., 1992. Dehydration melting and the generation of continental flood basalts. Nature 358, 57–59.

Green, D.H., 1973. Experimental melting studies on a model upper mantle composition at high pressure under water-saturated and water-undersaturated conditions. Earth Planet. Sci. Lett. 19, 37–53.

Hanson, G.N., 1980. Rare earth elements in petrogenetic studies of igneous systems. Annu. Rev. Earth Planet. Sci. 8, 371–406.

Hart, S.R., Dunn, T., 1993. Experimental cpx/melt partitioning of 24 trace elements. Contrib. Mineral. Petrol. 113, 1–8.

Harvey, P.K., Lovell, M.A., Brewer, T.S., Locke, J., Mansley, E., 1996. Measurement of thermal neutron absorption cross-section in selected geochemical reference materials. Geostand. Newsl. 20, 79–85.

Hawkesworth, C.J., Lightfoot, P.C., Fedorenko, V.A., Blake, S., Naldrett, A.J., Doherty, W., Gorbachev, N.S., 1995. Magma differentiation and mineralisation in the Siberian continental flood basalts. Lithos 34, 61–88.

Hawkesworth, C.J., Gallagher, K., Kirstein, L., Mantovani, M.S.M., Peate, D.W., Turner, S.P., 2000. Tectonic controls on magmatism associated with continental break-up: an example from the Paraná-Etendeka Province. Earth Planet. Sci. Lett. 179, 335–349.

Hergt, J.M., Peate, D.W., Hawkesworth, C.J., 1991. The petrogenesis of Mesozoic Gondwana low-Ti flood basalts. Earth Planet. Sci. Lett. 105, 134–148.

Jahn, B.-M., Gruau, G., Capdevila, R., Cornichet, J., Nemchin, A., Pidgeon, R., Rudnik, V.A., 1998. Archean crustal evolution of

the Aldan Shield, Siberia: geochemical and isotopic constraints. Precambrian Res. 91, 333–363.
King, S.D., Anderson, D.L., 1995. An alternative mechanism of flood basalt formation. Earth Planet. Sci. Lett. 136, 269–279.
King, S.D., Anderson, D.L., 1998. Edge-driven convection. Earth Planet. Sci. Lett. 160, 289–296.
Lightfoot, P.C., Naldrett, A.J., Gorbachev, N.S., Doherty, W., Fedorenko, V.A., 1990. Geochemistry of the Siberian Trap of the Noril'sk area, USSR, with implications for the relative contrubutions of crust and mantle to flood basalt magmatism. Contrib. Mineral. Petrol. 104, 631–644.
Lightfoot, P.C., Hawkesworth, C.J., Hergt, J., Naldrett, A.J., Gorbachev, N.S., Fedorenko, V.A., Doherty, W., 1993. Remobilisation of the continental lithosphere by a mantle plume: major-, trace-element, and Sr-, Nd-, and Pb-isotope evidence from picritic and tholeiitic lavas of the Noril'sk district, Siberian Trap, Russia. Contrib. Mineral. Petrol. 114, 171–188.
Mahoney, J.J., Storey, M., Duncan, R.A., Spencer, K.J., Pringle, M., 1993. Geochemistry and geochronology of the Ontong Java Plateau. In: Pringle, M., Sager, W., Sliter, W., Stein, S. (Eds.), The Mesozoic Pacific, Geology, Tectonics, and Volcanism vol. 77. American Geophysical Union Monograph, pp. 233–261.
McDonough, W.F., Sun, S.-S., 1995. The composition of the Earth. Chem. Geol. 120, 223–253.
McKenzie, D., Bickle, M.J., 1988. The volume and composition of melt generated by extension of the lithosphere. J. Petrol. 29, 625–679.
McKenzie, D., O'Nions, R.K., 1991. Partial melt distributions from inversion of rare earth element concentrations. J. Petrol. 32, 1021–1091.
Medvedev, A.Ya., Al'Mukhamedov, A.I., Kirda, N.P., 2003. Geochemistry of Permo–Triassic volcanic rocks of West Siberia. Russ. Geol. Geophys. 44, 86–100.
Naldrett, A.J., Lightfoot, P.C., Fedorenko, V.A., Doherty, W., Gorbachev, N.S., 1992. Geology and geochemistry of intrusions and flood basalts of the Noril'sk region, USSR, with implications for the origin of the Ni–Cu ores. Econ. Geol. 87, 975–1004.
Norman, M.D., Garcia, M.O., 1999. Primitive magmas and source characteristics of the Hawaiian plume: petrology and geochemistry of shield picrites. Earth Planet. Sci. Lett. 168, 27–44.
Pavlenkova, G.A., Priestley, K., Cipar, J., 2002. 2D model of the crust and uppermost mantle along rift profile, Siberian craton. Tectonophysics 355, 171–186.
Peate, D.W., Hawkesworth, C.J., 1996. Lithospheric to asthenospheric transition in low-Ti flood basalts from southern Paraná, Brazil. Chem. Geol. 127, 1–24.
Peterson, J.A., Clarke, J.W., 1991. Geology and Hydrocarbon Habitat of the West Siberian Basin, vol. 32. America Association of Petroleum Geologists, Tulsa, Oklahoma, p. 93.
Reichow, M.K., Saunders, A.D., White, R.V., Pringle, M.S., Al'Mukhamedov, A.I., Medvedev, A.Ya., Kirda, N.P., 2002. $^{40}Ar/^{39}Ar$ dates from the West Siberian Basin: Siberian Flood Basalt Province doubled. Science 296, 1846–1849.
Renne, P.R., Basu, A.R., 1991. Rapid eruption of the Siberan traps flood basalts at the Permo–Triassic boundary. Science 253, 176–179.
Richards, M.A., Duncan, R.A., Courtillot, V.E., 1989. Flood basalts and hot-spot tracks: plume heads and tails. Science 246, 103–107.
Robinson, J.A., Wood, B.J., 1998. The depth of the spinel to garnet transition at the peridotite solidus. Earth Planet. Sci. Lett. 164, 277–284.
Salters, V.J.M., Stracke, A., 2004. Composition of the depleted mantle. Geochem. Geophys. Geosyst. 5 (5), Q05004, doi:10.1029/2003GC000597.
Saunders, A.D., Tarney, J., 1984. Geochemical characteristics of basaltic volcanism within back-arc basins. In: Kokelaar, B.P., Howells, M.F. (Eds.), Marginal Basin Geology: Volcanic and Associated Sedimentary and Tectonic Processes in Modern and Ancient Marginal Basins, vol. 16. Geological Society of London Special Publication, London, pp. 59–76.
Saunders, A.D., Storey, M., Kent, R.W., Norry, M.J., 1992. Consequences of plume–lithosphere interactions. In: Storey, B.C., Alabaster, T., Pankhurst, R.J. (Eds.), Magmatism and the Causes of Continental Breakup, vol. 68. Geological Society of London Special Publication, London, pp. 41–60.
Saunders, A.D., England, R.W., Reichow, M.K., White, R.V., 2005. A mantle plume origin for the Siberian Traps: 1. Uplift and extension in the West Siberian Basin. Lithos 79, 407–424.
Self, S., Thordarson, Th., Keszthelyi, L., 1997. Emplacement of continental flood basalt lava flows. In: Mahoney, J.J., Coffin, M.F. (Eds.), Large Igenous Provinces: Continental, Oceanic, and Planetary Flood Volcanism, vol. 100. American Geophysical Union Monograph, Washington, DC, pp. 381–410.
Self, S., Keszthelyi, L., Thordarson, Th., 1998. The importance of Pahoehoe. Earth Planet. Sci. Lett. 26, 81–110.
Sharma, M., 1997. Siberian Traps. In: Mahoney, J.J., Coffin, M.F. (Eds.), Large Igneous Provinces: Continental, Oceanic, and Planetary Flood Volcanism, vol. 100. American Geophysical Union Monograph, Washington, DC, pp. 273–295.
Sharma, M., Basu, A.R., Nesterenko, G.V., 1991. Nd–Sr isotopes, petrochemistry, and origin of the Siberian flood basalts. USSR Geochim. Cosmochim. Acta 55, 1183–1192.
Sharma, M., Basu, A.R., Nesterenko, G.V., 1992. Temporal Sr-, Nd- and Pb-isotopic variations in the Siberian flood basalts: implications for the plume-source characteristics. Earth Planet. Sci. Lett. 113, 365–381.
Storey, M., Mahoney, J.J., Saunders, A.D., 1997. Cretaceous basalts in Madagascar and the transition between plume and continental lithosphere mantle sources. In: Mahoney, J.J., Coffin, M.F. (Eds.), Large Igneous Provinces: Continental, Oceanic, and Planetary Flood Volcanism, vol. 100. American Geophysical Union Monograph, Washington, DC, pp. 95–122.
Surkov, V.S., (Ed.), 1995. Atlas of paleotectonic and paleogeological-landscape maps of hydrocarbon provinces of Siberia. SNIIG-GIMS, Petroconsultants, Novosibirsk, 222 pp. and 30 enclosures.
Tejada, M.L.G., Mahoney, J.J, Castillo, P.R., Ingle, S.P., Sheth, H.C., Weis, D., 2004. Pin-pricking the elephant (ODP LEG 192): Pb–Sr–Hf–Nd isotopic evidence on the origin of the Ontong Java Plateau. In: Fitton, J.G., Mahoney, J.J., Wallace, P.J., Saunders, A.D. (Eds.), Origin and Evolution of the Ontong Java Plateau, vol. 229. Geological Society of London Special Publication, London, pp. 133–150.

Turner, S., Hawkesworth, C.J., 1995. The nature of the sub-continental mantle: constraints from the major-element composition of continental flood basalts. Chem. Geol. 120, 295–314.

Vernikovsky, V.A., Neimark, L.A., Ponomarchuk, V.A., Vernikovskaya, A.E., Kireev, A.D., Kuz'min, D.S., 1995. Geochemistry and age of collision granitoids and metamorphites of the Kara microcontinent (northern Taimyr). Russ. Geol. Geophys. 36 (12), 46–60.

Vernikovsky, V.A., Pease, V.L., Vernikovskaya, A.E., Romanov, A.P., Gee, D.G., Travin, A.V., 2003. First report of early Triassic A-type granite and syenite intrusions from Taimyr: product of the northern Eurasian superplume? Lithos 66, 23–36.

Walter, M.J., 1998. Melting of garnet peridotite and the origin of Komatiite and depleted lithosphere. J. Petrol. 39, 29–60.

Watson, S., McKenzie, D., 1991. Melt generation by plumes: a study of Hawaiian volcanism. J. Petrol. 32, 501–537.

Weaver, B.L., Tarney, J., 1984. Empirical approach to estimating the composition of the continental crust. Nature 310, 575–577.

Wedepohl, K.H., 1995. The composition of the continental crust. Geochim. Cosmochim. Acta 59, 1217–1232.

Westphal, M., Gurevitch, E.L., Samsonov, B.V., Feinberg, H., Pozzi, J.P., 1998. Magnetostratigraphy of the lower Triassic volcanics from deep drill SG6 in western Siberia: evidence for long-lasting Permo–Triassic volcanic activity. Geophys. J. Int. 134, 254–266.

White, R.S., McKenzie, D.P., 1989. Magmatism at rift zones: the generation of volcanic continental margins and flood basalts. J. Geophys. Res. 94, 7685–7729.

Wooden, J.L., Czamanske, G.K., Fedorenko, V.A., Arndt, N.T., Chauvel, C., Bouse, R.M., King, B.W., Knight, R.J., Siems, D.F., 1993. Isotopic and trace-element constraints on mantle and crustal contributions to Siberian continental flood basalts, Noril'sk area, Siberia. Geochim. Cosmochim. Acta 57, 3677–3704.

Ziegler, P.A., 1992. Plate tectonics, plate moving mechanisms and rifting. Tectonophysics 215, 9–34.

Zolotukhin, V.V., Al'Mukhamedov, A.I., 1988. Traps of the Siberian platform. In: Macdougall, J.D. (Ed.), Continental Flood Basalts. Kluwer Academic, Amsterdam, pp. 273–310.

Zonenshain, L.P., Kuzmin, M.I., Natapov, L.M., 1990. Geology of the USSR: a plate tectonic synthesis. Am. Geophys. Union Geodyn. Ser. 21, 242.